TECTONICS, VOL. 20, NO. 5, PAGES, 601-624 OCTOBER 2001

A reappraisal of the Sibson-Scholz fault zone model: The nature of the frictional to viscous ("brittle-ductile") transition along a long-lived, crustal-scale fault, Outer Hebrides, Scotland

J. Imber, [1] R. E. Holdsworth, and C. A. Butler

Reactivation Research Group, Department of Geological Sciences, University of Durham, Durham, England, UK

R. A. Strachan

Geology (BMS), Oxford Brookes University, Headington, Oxford, England, UK

Abstract. The widely cited Sibson-Scholz conceptual fault zone model suggests that seismically active, upper crustal brittle faults pass downward across a predominantly thermally controlled transition at 10-15 km depth into ductile shear zones in which deformation occurs by aseimic viscous creep. The crustal-scale Outer Hebrides Fault Zone (OHFZ) in NW Scotland has been described as the type example of such a continental fault zone. It cuts Precambrian basement gneisses and is deeply exhumed, allowing direct study of the deformation products and processes that occur across a wide range of crustal depths. A number of fault rock assemblages are recognized to have formed during a long-lived displacement history lasting in excess of 1000 Myr. During Caledonian movements that are recognized along much of the 190 km onshore fault trace, brittle, cataclasite-bearing faults in the west of the OHFZ are unequivocally overprinted to the east by a younger fabric related to a network of ductile shear zones. Field observations and regional geochronological data demonstrate that there is no evidence for reheating of the fault zone due to thrust-related crustal thickening or shear heating. Microstructural observations show that the onset of viscous deformation was related to a major influx of hydrous fluids. This led to retrogression, with the widespread development of new fine-grained phyllosilicate-bearing fault rocks ("phyllonites"), and the onset of fluid-assisted, grain size-sensitive diffusional creep in the most highly deformed and altered parts of the fault zone. Phyllonitic fault rocks also occur in older, more deeply exhumed parts of the fault zone, implying that phyllonitization had previously occurred at an earlier stage and that this process is possible over a wide temperature (depth) range within crustal-scale faults. Our data provide an observational basis for recent theoretical and experimental studies which suggest that crustal-scale faults containing interconnected networks of phyllosilicate-bearing fault rocks will be characterized by long-term relative weakness and shallow (~5 km) frictional-viscous transition zones. Similar processes acting at depth may provide an explanation for the apparent weakness of presently active structures such as the San Andreas Fault.

1. Introduction

Studies of natural and experimentally deformed fault rocks suggest that strain in the Earth's crust is accommodated by a number of different deformation mechanisms [e.g., *Sibson*, 1977a; *Handy*, 1989; *Schmid and Handy*, 1991; *Snoke et al.*, 1988; *Rutter et al.*, 2001]. At relatively low temperatures and pressures typical of the upper crust, deformation is characterized by pressure-sensitive (dilatant) flow involving fracturing [*Lloyd and Knipe*, 1992], frictional grain boundary sliding [*Maltman*, 1994], cataclasis [*Engelder*, 1974], and frictional melting [*Sibson*, 1975]. At greater depths, increases in temperature and pressure favor the operation of thermally activated (i.e., temperature sensitive) "viscous creep" processes (in the sense of *Schmid and Handy* [1991]) such as crystal plasticity [*Drury and Urai*, 1990; *Hirth and Tullis*, 1992] and grain size-sensitive diffusion creep [*Rutter*, 1983; *Schmid and Handy*, 1991]. These observations together with measurements of microseismic activity in different continental heat flow provinces [*Sibson*, 1982] led to the widely accepted Sibson-Scholz "conceptual fault zone model". This model envisages an upper, seismogenic zone deforming by frictional flow and a lower, aseismic zone deforming predominantly by viscous processes [*Sibson*, 1977a, 1983; *Scholz*, 1988] (Figure 1a). The two flow regimes are separated by the "frictional-viscous (or brittle-ductile) transition zone" [*Schmid and Handy*, 1991], a region of complex, alternating behavior, generally believed to coincide with the main load-bearing region of the crust (Figure 1a) [*Sibson*, 1983]. For "average" quartzo-feldspathic crust the frictional-viscous transition is expected to occur in the midcrust, at ~10-15 km depth, although its exact depth range will depend on a number of factors, including ambient geothermal gradient, strain rate, mode of faulting, pore-fluid pressure [*Sibson*, 1983; *Scholz*, 1988], the chemical effects of fluids in the crust [*Tullis and Yund*, 1980], and fault rock composition, mineralogy, and microstructure [*White et al.*, 1986; *Handy*, 1989]. The depth at which the frictional-viscous transition occurs is likely to influence the behavior of crustal-scale faults and could, in prin-

[1] Now at Fault Analysis Group, Department of Geology, University College Dublin, Dublin, Ireland.

Paper number 2000TC001250.
0278-7407/01/2000TC001250$12.00

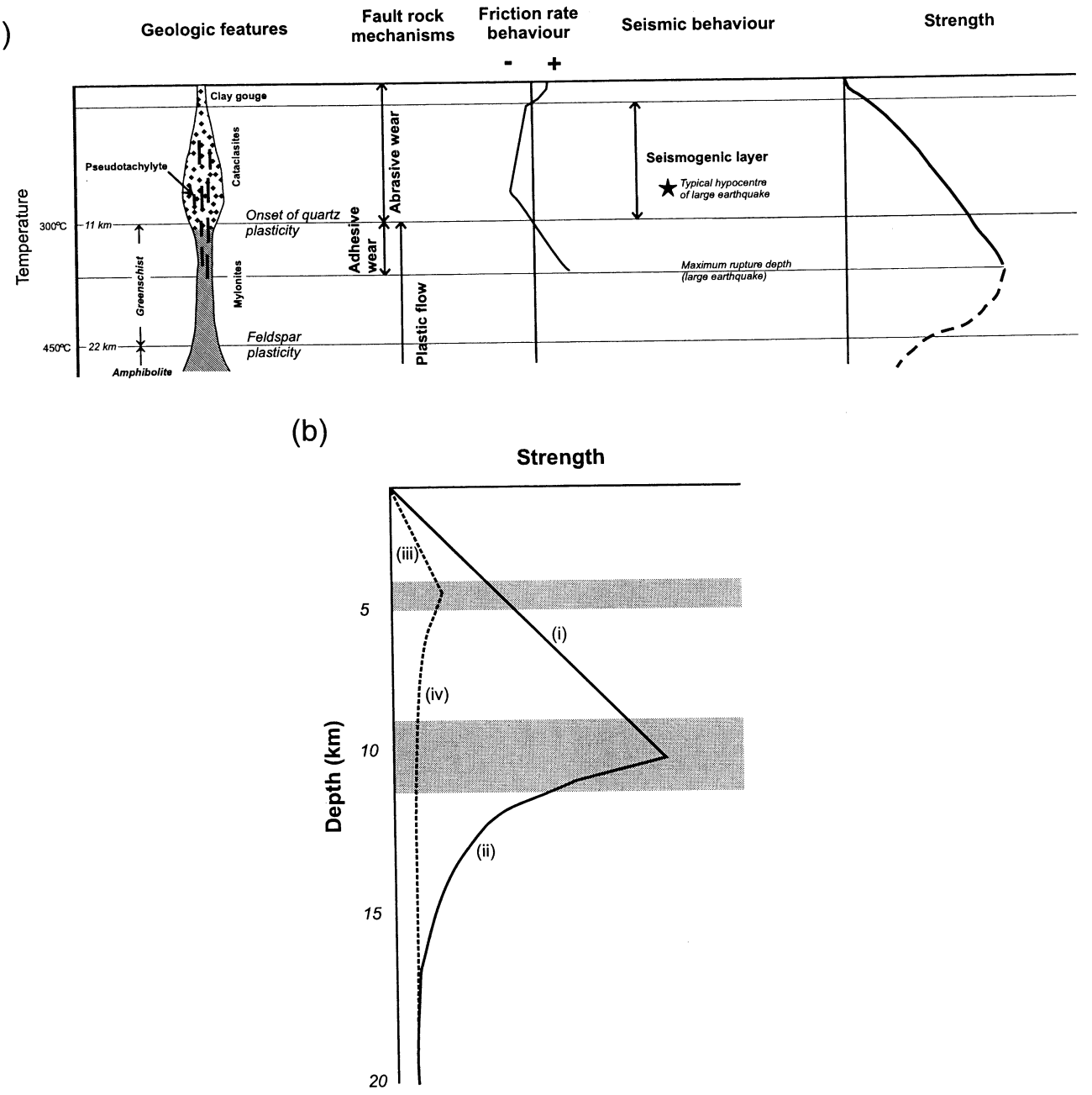

Figure 1. Previously published conceptual fault zone models. (a) The Sibson-Scholz model for a vertical fault developed in quartzo-feldspathic crust [after *Scholz,* 1988]. Note that if friction rate behavior is positive, sliding is velocity strengthening, and if it is negative, sliding is velocity weakening [*Scholz*, 1988]. (b) Schematic strength profiles for vertical faults developed in quartzo-feldspathic (curves i and ii) and phyllosilicate-bearing (dashed curves iii and iv) rocks (see *Janecke and Evans* [1998] for details). The shaded areas represent the approximate position of the frictional-viscous transition zone for faults cutting these two rock types.

ciple, impact on the nature of fault slip [*Sibson*, 1983], the depth to the base of the seismogenic layer [*Scholz*, 1990], and the amount of heat production due to shearing in the frictional, upper part of the crust [*Lachenbruch and Sass*, 1992].

Schmid and Handy [1991] proposed that the operation of grain size-sensitive deformation mechanisms could be triggered by (1) cataclasis in the frictional regime, (2) dynamic recrystallization in the viscous regime, or (3) syntectonic metamorphic reactions in either the frictional or viscous regimes. Such changes can, in principle, lead to significant narrowing and shallowing of the frictional-viscous transition zone compared to the "standard" Sibson-Scholz models [*Schmid and Handy*, 1991]. Subsequent authors have presented models in which extreme shallowing of the frictional-viscous transition occurs because of a strain-induced switch to grain size-sensitive diffusion creep in the presence of an

aqueous fluid and/or the development of mechanically weak, phyllosilicate-bearing fault rocks in the midcrust [*Shea and Kronenberg*, 1992; *Janecke and Evans*, 1993; *Imber et al.*, 1997; *Stewart et al.*, 2000; *Holdsworth et al.*, 2001; cf. *Wibberley*, 1999] (Figure 1b). Theoretical studies by *Wintsch et al.* [1995] show that syntectonic metamorphic reactions between framework silicates (e.g., feldspar) and Mg-rich aqueous pore fluids can produce highly foliated, phyllosilicate-bearing gouges and mylonites (a process we refer to here as "phyllonitization") over a wide depth range within crustal-scale faults. Their model implies that the transition from frictional to viscous behavior occurs at depths of less than ~5 km in faults containing interconnected networks of phyllosilicate-rich fault rocks [see *Wintsch et al.*, 1995, figure 4]. The conclusions of this and other studies are, however, based on the assumption that limited outcrop, microstructural, and experimental data can be extrapolated across the entire crustal section. Thus there is a clear need to test these proposals with observations of natural fault rocks and structures developed over a range of midcrustal "paleodepths" within a single, crustal-scale fault zone.

Reactivated faults and shear zones exposed in the deeply exhumed parts of ancient orogenic belts present opportunities to examine directly fault zone processes that operate at different depths in the continental crust [*Grocott*, 1977; *Holdsworth et al.*, 1997]. In this study, we examine the distribution, relative ages, kinematics, and microfabrics of strongly foliated, phyllosilicate-bearing mylonites (here termed "phyllonites") (in the sense of *O'Hara* [1988] and *Hippertt* [1994a, 1994b, 1998]) and their precursor fault rocks that are inferred to have developed above and below the level of an ancient, evolving frictional-viscous transition in an exhumed basement fault zone: the Outer Hebrides Fault Zone (OHFZ), Scotland (Figure 2a). The study area is especially appropriate as *Sibson's* [1977a] original conceptual fault zone model was largely based upon field studies of fault rocks from this crustal-scale structure [*Sibson*, 1977b]. Our findings suggest that the widely accepted conceptual fault zone models of *Sibson* [1977a; 1983] and *Scholz* [1988] are not appropriate for the Outer Hebrides Fault Zone, in particular, and may not be appropriate for "mature" (i.e., long-lived), crustal-scale faults, in general. In section 4, we discuss briefly the implications of our results for geophysically observed patterns of seismicity and heat flow around active, crustal-scale faults and present a revised conceptual model for faults with shallow, tectonically modified frictional to viscous transition zones.

2. Geological Background and Overview of the Outer Hebrides Fault Zone

The OHFZ crops out for ~190 km along the east coast of the Outer Hebrides, Scotland [*Sibson*, 1977b; *Lailey et al.*, 1989; *Butler*, 1995; *Butler et al.*, 1995; *Imber et al.*, 1997; *Imber*, 1998; *MacInnes et al.*, 2000] (Figure 2a). The fault zone dips at 20-30° toward the east or SE and deep (15 s two-way time (TWT)), two-dimensional (2-D) seismic reflection profiles suggest that the fault intersects and may offset the Moho at ~25 km depth [*Smythe et al.*, 1982; *Peddy*, 1984]. Interpretations of borehole [*Binns et al.*, 1974] and conventional (6 s TWT) 2-D seismic reflection data show that packages of late Proterozoic ("Torridon Group", dated at ca. 1000 Ma [*Strachan and Holdsworth*, 2000]) and Carboniferous-age sediments thicken from east to west across the Minch and Sea of the Hebrides Basins and reach their maximum thickness in the immediate hanging wall of the OHFZ [*Stein*, 1988, 1992] (Figure 2b). During the Permo-Triassic, the western margin of these hanging wall basins was defined by the Minch Fault, an east dipping growth fault which branches up from and partially reactivates the underlying Outer Hebrides Fault Zone (Figures 2a and 2b) [*Stein*, 1988]. These offshore observations show the OHFZ to be a crustal-scale structure that was active during Proterozoic, Carboniferous, and Mesozoic extension in NW Scotland.

The exceptional exposure onshore of the OHFZ probably reflects uplift in the footwall of the Minch Fault, combined with the effects of later regional uplift caused by underplating of basalts below this part of NW Scotland during the opening of the North Atlantic [*Brodie and White*, 1994; *Roberts and Holdsworth*, 1999]. The exposed fault zone is between 1 and 6 km thick and is seen to crosscut preexisting, mainly amphibolite facies basement gneisses of the Archaean to Palaeoproterozoic Lewisian Complex [*Fettes and Mendum*, 1987]. A suite of K-Ar and Rb-Sr radiometric age dates have been obtained from gneisses preserved in the footwall of the Outer Hebrides Fault Zone [*Lambert et al.*, 1970; *Moorbath et al.*, 1975; *Cliff and Rex*, 1989; *Fettes et al.*, 1992], providing some constraint on the "high-temperature" (greater than ~300°C) evolution of the Lewisian country rocks. Gneisses which crop out to the south of the NW-SE trending South Harris Shear Zones (SHSZ, Figure 2a) typically yield K-Ar hornblende ages of between 1650 and 2100 Ma, Rb-Sr biotite ages of between 1340 and 1630 Ma, and K-Ar biotite ages of between 1500 and 1750 Ma [*Moorbath et al.*, 1975; *Cliff and Rex*, 1989] (see Figure 3a for details). These ages record cooling and exhumation of the gneisses from a maximum burial depth of ~20 km following Proterozoic ("Laxfordian", ca. 1700 Ma) deformation and metamorphism [*Watson*, 1977; *Fettes et al.*, 1992] (Figure 3a). Gneisses which crop out to the north of the SHSZ (Figure 2a), however, yield two distinct groups of Rb-Sr biotite ages (Figure 3b). Most samples produce "Grenvillian" ages of between 950 and 1300 Ma, but gneisses which preserve either granulite facies mineral assemblages or primary (igneous) biotite crystals yield significantly older ages ranging from 1550 to 1670 Ma [*Cliff and Rex*, 1989] (Figure 3b). The latter overlap with the K-Ar biotite ages obtained from gneisses to the south of the SHSZ and thus record cooling following Laxfordian deformation and metamorphism (Figure 3). *Cliff and Rex* [1989] attribute Grenvillian resetting of the Rb-Sr biotite ages to reheating and cooling of the crust in the northern Outer Hebrides caused by kilometer-scale, north side up dextral-oblique [*Butler*, 1995] displacements across the South Harris Shear Zones at around 1100 Ma. Grenvillian metamorphism is the youngest tectonothermal "event" to be recorded in the footwall of the OHFZ by either the K-Ar or Rb-Sr systems (Figure 3).

Overprinting relationships between different fault rocks and structures preserve evidence for at least five fault-related deformation events along the onshore trace of the OHFZ to the north of the South Harris Shear Zones (the "northern segment", Figure 2a and Table 1) [*Butler*, 1995; *Butler et al.*,

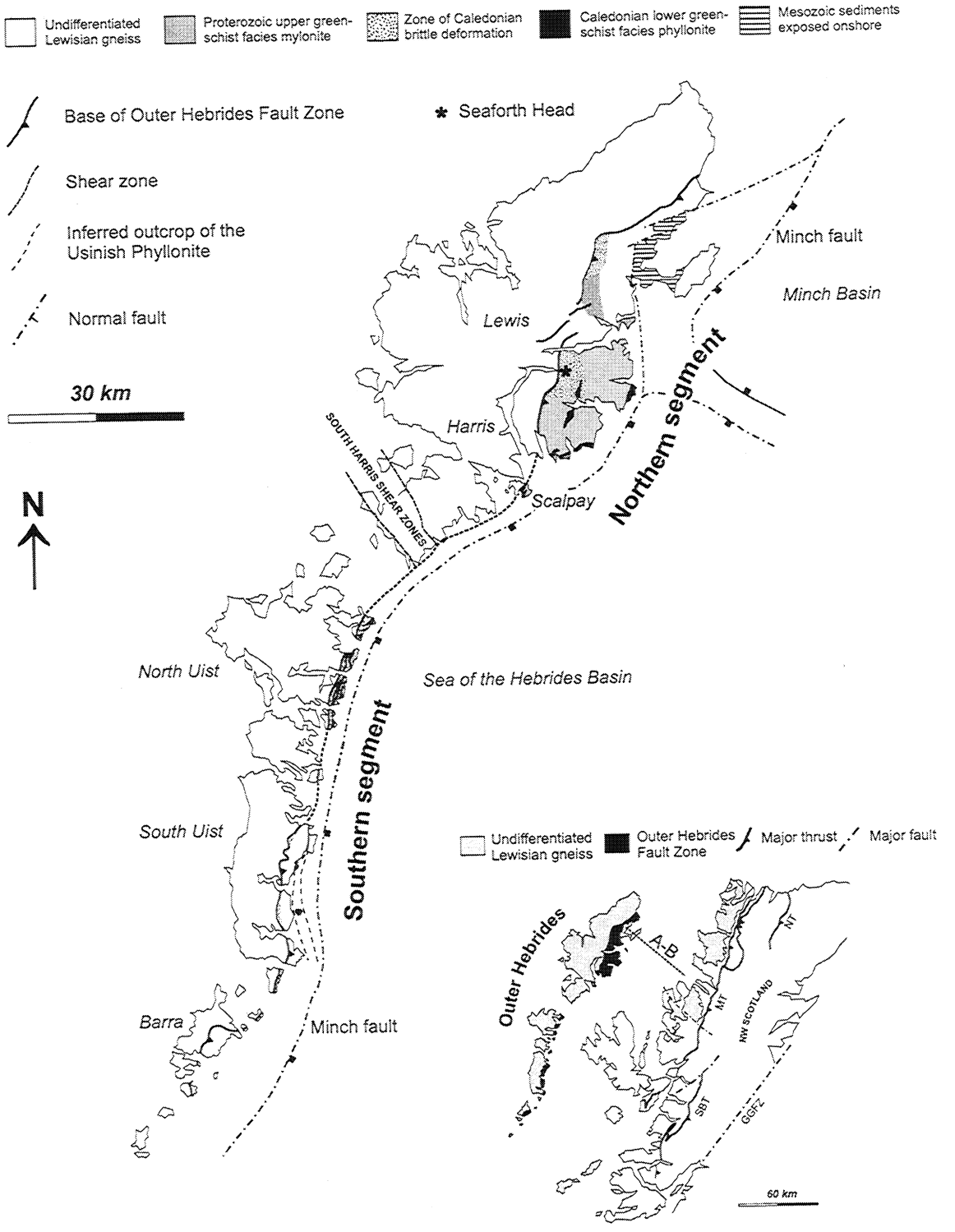

Figure 2. (a) Simplified geological map showing the general distribution of fault rocks within the Outer Hebrides Fault Zone, major offshore basins and the main basin-bounding faults. Map complied from *Sibson* [1977b], *Fettes et al.* [1992], *Butler* [1995], and *Imber* [1998]. Inset shows the Outer Hebrides Fault Zone in relation to major Caledonian structures exposed on the Scottish mainland. MT, Moine Thrust; NT, Naver Thrust; SBT, Sgurr Beag Thrust; GGFZ, Great Glen Fault Zone. Line A-B shows location of (b) geoseismic cross section across the Minch Basin from *Stein* [1992].

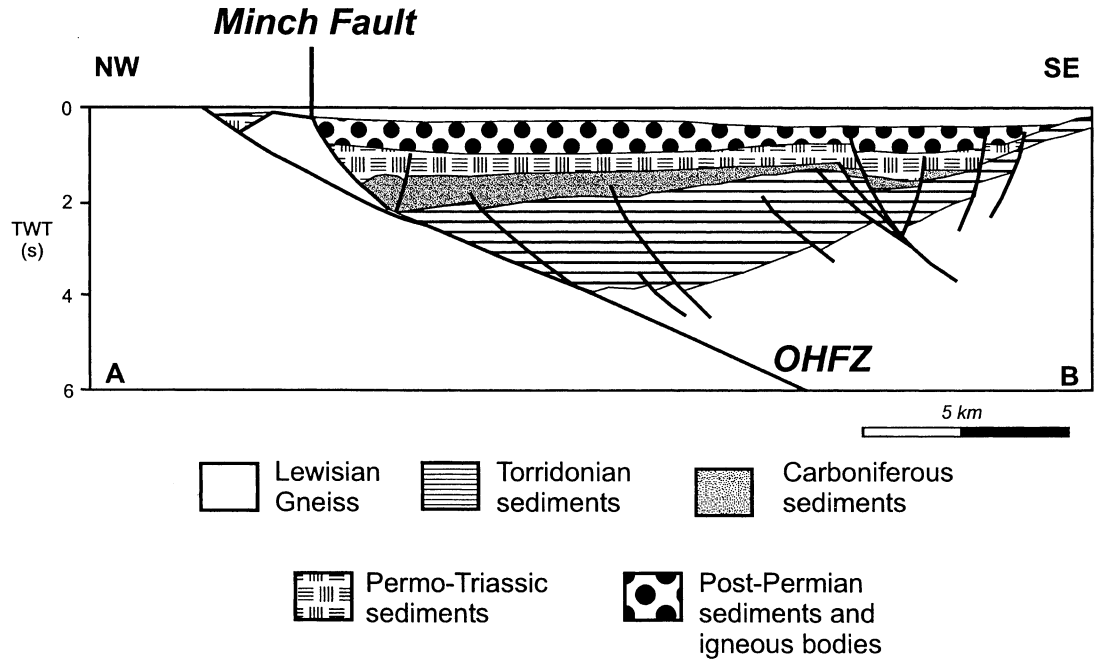

Figure 2. (continued)

1995; *Imber*, 1998]. Starting with the oldest event, these are (1) top to the NW thrusting in a broad ductile shear zone, (2) brittle top to the W thrusting, (3) sinistral strike slip in a network of macroscopically ductile shear zones, (4) brittle-ductile extension, and (5) brittle top to the E extension. The earliest recorded deformation event is top to the NW thrusting associated with the development of upper greenschist to lower amphibolite facies phyllonites and mylonites in a broad (less than 6 km thick), east to SE dipping shear zone. The shear zone is well exposed at Seaforth Head and on the island of Scalpay (Figure 2a) where phyllonites and mylonites overprint and rework Laxfordian-age pegmatite veins. These thrust-related mylonitic fault rocks do not, however, crop out along the southern segment of the OHFZ (i.e., to the south of the SHSZ; Figure 2a), implying that the southern continuation of the shear zone was displaced to the NW (now offshore) during Grenvillian dextral-oblique movements across the South Harris Shear Zones (see discussion by *Butler* [1995]). We conclude therefore that early, top to the NW thrusting in the Outer Hebrides occurred post-1700 but pre-1100 Ma (Table 1 and Figure 3). Using strain estimates obtained from measurements of boudinaged basic layers, shortening across buckle folds, and the orientation of the mylonitic foliation relative to the "sheet dip" of the fault zone, *Sibson* [1977b] calculated a minimum updip displacement of between 1.8 and 3 km across the shear zone. Assuming a dip of 30°, these estimates imply a minimum, thrust-related increase in crustal thickness of between 1 and 2 km. Temperatures during Proterozoic thrusting have been constrained using geothermometers based on the compositions of syntectonic minerals preserved in mylonites at Seaforth Head and range from 535° ± 50°C [*Fettes and Mendum*, 1987] to 520° ± 60°C [*White*, 1996] (see Figure 3 for details).

The western margin of the Proterozoic shear zone is overprinted by arrays of cataclasite- and pseudotachylyte-bearing faults and crush zones that we infer to have developed during top to the west Caledonian thrusting (Figure 2a). Farther east, however, the intensity of brittle deformation appears to decrease, and both the Proterozoic phyllonites and mylonites and the Caledonian cataclasites and pseudotachylytes are reworked by a number of narrow (< 500 km thick), north to NE trending, lower greenschist facies sinistral strike-slip-related phyllonitic shear zones. A sample of lower greenschist facies phyllonite from SE Scalpay (Figure 2a) produced a whole-rock K-Ar age of 394 ± 16 Ma (D. C. Rex as discussed by *Sibson* [1977b]), consistent with late Caledonian phyllonitization and greenschist facies metamorphism along the northern segment of the OHFZ [*Butler et al.*, 1995]. Displacement and paleotemperature estimates pertaining to sinistral strike slip and lower greenschist facies phyllonitization are discussed below.

The phyllonitic shear zones are locally cut by brittle, foliation-parallel detachment faults, and the macroscopically ductile, strike-slip-related fabrics are themselves deformed by "cascades" of downdip (i.e., south to SE) verging, centimeter- to meter-scale folds. The detachment and fold geometries are consistent with the phyllonitic shear zones having been reactivated and reworked during regional, top to the south or SE extension along the northern segment of the OHFZ [*Butler et al.*, 1995; *Imber*, 1998; cf. *Fettes et al.*, 1992]. Isotopic age dates are not available to directly constrain the age of brittle-ductile dip-slip extension, but evidence from apatite fission track analysis (see below) suggests that a pre-Devonian (i.e., pre-400 Ma) age is likely. The final phase of deformation recorded along the northern segment of the OHFZ was the development of steep, east and SE dipping normal faults.

These occur in the footwall of the Minch Fault (Figure 2a) and mark the western limit of Permo-Triassic (and possibly Carboniferous) sedimentation along the margins of the Minch Basin [*Steel and Wilson*, 1975] (Figure 2b). Permo-Triassic sandstones and conglomerates, which locally crop out in NE Lewis (Stornoway Formation, Figure 2a), contain abundant clasts of locally derived Lewisian gneiss, cataclasite, and pseudotachylyte [*Sibson*, 1977b]. This observation implies that Caledonian-age fault rocks were at the surface and being eroded during the Permo-Triassic. Fission track ages obtained from apatite grains separated from clasts of gneiss preserved in the Stornoway Formation [*Lewis et al.*, 1992; *Thomson et al.*, 1999] and from in situ gneisses preserved in the footwall of the OHFZ on Harris [*Lewis et al.*, 1992] range from 200 to 500 Ma but cluster around 200 and 300 Ma (Figure 3a). *Lewis et al.* [1992] interpret these and track length distribution data to mean that the gneisses began to cool from maximum temperatures of ~110°C at the beginning of the Devonian or earlier (~400 Ma), and they suggest that at that time the present-day erosion surface was buried beneath no more than 3-4 km of overburden. These apatite fission track ages provide useful constraints on the thermal evolution of the OHFZ and are discussed further in section 4.

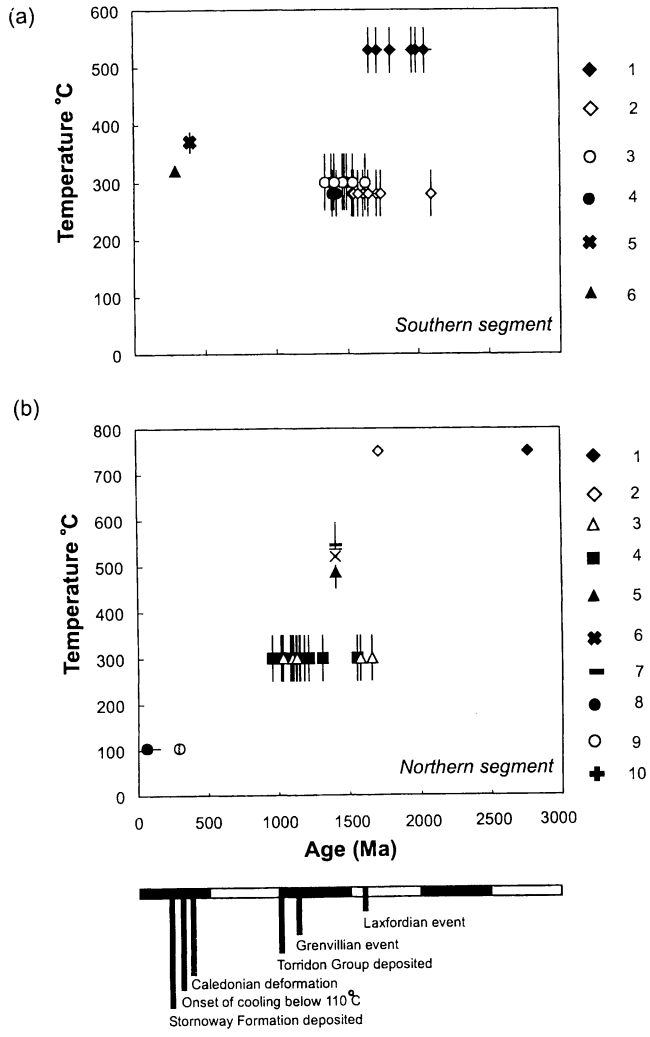

Overprinting relationships define at least four fault-related deformation events along the onshore trace of the OHFZ to the south of the South Harris Shear Zones (the "southern segment", Figure 2a and Table 1). Starting with the oldest event, these are (1) brittle top to the west thrusting, (2) sinistral strike slip across a network of macroscopically ductile shear zones, (3) brittle-ductile top to the east or SE extension, and (4) brittle top to the NE or east strike slip/extension [*Butler*, 1995; *Butler et al.*, 1995; *Imber*, 1998]. The similarities in kinematics, style of deformation, and in some cases, isotopic ages have led previous authors [*Butler*, 1995; *Imber*, 1998] and ourselves to correlate these movements with the four

Figure 3. Diagram summarizing existing paleotemperature and isotopic age data for footwall protoliths and selected fault rocks in the Outer Hebrides. Blocking temperatures are from a compilation by *Fowler* [1990]. (a) Data from the southern segment: 1, K-Ar dates obtained from hornblende grains preserved in gneisses from North and South Uist, Benbecula, and Barra [*Moorbath et al.*, 1975]; 2, K-Ar dates obtained from biotite grains preserved in gneisses from North and South Uist, Benbecula, and Barra [*Moorbath et al.*, 1975]; 3, Rb-Sr dates obtained from biotite grains preserved in gneisses from the South Harris Granulite Facies Terrain [*Cliff and Rex*, 1989]; 4, K-Ar dates obtained from biotite grains preserved in late Laxfordian microdiorite bodies, Garry a-siar, Benbecula [*Fettes et al.*, 1992]; 5, temperature estimate from the homogenization temperature of primary fluid inclusions in a syntectonic quartz vein within the Usinish Phyllonite, South Uist [*Osinski et al.*, 2001] (age estimated from geological constraints, see text for details); 6, Rb-Sr date obtained from biotite grains preserved in posttectonic quartz-diorite and camptonite dykes which crosscut the OHFZ on South Uist and Barra [*Fettes et al.*, 1992]. (b) Data from the northern segment. 1, U-Pb date on zircons in tonalitic gneiss from Harris [*Pidgeon and Aftalion*, 1972]; 2, U-Pb date on zircons in rocks from the Uig Hills-Harris granite complex, Lewis and Harris [*van Breemen et al.*, 1971]; 3, Rb-Sr dates on biotites in gneisses to the north of the south Harris migmatite complex [*Cliff and Rex*, 1989]; 4, Rb-Sr dates on biotites in gneisses from the Harris migmatite complex [*Cliff and Rex*, 1989]; 5, temperature estimated from the orthoclase-microcline transformation in feldspar grains preserved within the Proterozoic shear zone, Seaforth Head, Lewis [*White*, 1996] (age estimated from geological constraints, see text for details); 6, temperature estimated from plagioclase and amphibole compositions in mylonites preserved within the Proterozoic shear zone, Seaforth Head, Lewis [*White*, 1996] (age estimated from geological constraints, see text for details); 7, temperature estimated using garnet-biotite geothermometer mylonites preserved within the Proterozoic shear zone, Seaforth Head, Lewis [*Fettes and Mendum*, 1987] (age estimated from geological constraints, see text for details); 8, mean fission track age obtained from apatite grains in a gneissose boulder preserved within Stornoway Formation conglomerate, Lewis [*Thomson et al.*, 1999]; 9, mean fission track age obtained from apatite grains in a gneissose pebble preserved within Stornoway Formation conglomerate, Lewis [*Lewis et al.*, 1992]; 10, mean fission track age obtained from apatite grains in in situ gneisses, south Harris [*Lewis et al.*, 1992]. Note that the mean fission track age does not convey the same information as the track length distribution (not shown) [*Lewis et al.*, 1992].

Table 1. Kinematic History of the Outer Hebrides Fault Zone (OHFZ) and South Harris Shear Zones (SHSZ).

Northern Segment (North of SHSZ)	Southern Segment (South of SHSZ)
Top to NW thrusting: broad shear zone containing upper greenschist to lower amphibolite facies mylonite and phyllonite; post-1700 Ma, but pre-1100 Ma age inferred	Absent ("tectonically excised" by SHSZ ?) - -
Dextral oblique shear across the SHSZ [Butler, 1995]: associated with relative uplift and resetting of R-Sr biotite ages in north Harris and Lewis [Cliff and Rex 1989]; ca. 1100 Ma age inferred	
Top to the E extension (?): Proterozoic (Torridon Group) sediments, which thicken toward the hanging wall of the OHFZ, are preserved in the Minch Basin, implying that extension was accommodated by movements along the OHFZ; fault rocks/structures related to this Proterozoic event do not crop out onshore in the Outer Hebrides; ca. 1000 Ma age inferred	Top to the E extension (?): Proterozoic (Torridon Group) sediments, which thicken toward the hanging wall of the OHFZ, are preserved in the Sea of the Hebrides Basin, implying that extension was accommodated by movements along the OHFZ; fault rocks/structures related to this Proterozoic event do not crop out onshore in the Outer Hebrides; ca. 1000 Ma age inferred
Top to NW brittle thrusting: cataclasites and pseudotachylyte-bearing faults; Late Caledonian age (ca. 430 Ma) inferred	Top to NW brittle thrusting: pseudotachylyte-bearing faults and crush zones; Late Caledonian age (ca. 430 Ma) inferred
Sinistral, top to NE strike-slip: narrow, lower greenschist facies phyllonitic shear zones; Late Caledonian age (ca. 400 Ma) inferred	Sinistral, top to NE strike-slip: narrow, lower greenschist facies phyllonitic shear zones; Late Caledonian age (ca. 400 Ma) inferred
Top to south or east dipslip: reworking of phyllonitic fabrics, with localized brittle deformation on foliation-parallel faults; ? Late Caledonian	Top to east or SE dipslip: reworking of phyllonitic fabrics, with localized brittle deformation on foliation-parallel faults; ? Late Caledonian
Dipslip extension: east-dipping normal faults; ?Carboniferous to Mesozoic age inferred	Top to NE and east strike-slip/extension: shallowly east to SE dipping faults; pre-Carboniferous age inferred

youngest deformation events observed along the northern segment of the OHFZ (Table 1).

The earliest phase of deformation is top to the west thrusting accommodated by brittle faulting, cataclasis, and pseudotachylyte generation (see *Coward* [1972] and *Sibson* [1977b] but see discussion by *Osinski et al.* [2001]). Ar-Ar dates obtained from the matrix of a pseudotachylyte vein preserved in the immediate footwall of the OHFZ yield a weighted mean age of 430 ± 3 Ma (1σ), consistent with Caledonian thrusting across the Outer Hebrides Fault Zone [*Kelley et al.*, 1994]. *Coward* [1969] inferred Caledonian thrust displacements of between 2 and 3 km by applying empirical displacement-thickness relationships to the pseudotachylyte-ultracataclasite crush zones which crop out on South Uist. In contrast, *Sibson* [1977b] calculated 4-8 km slip from the offset of a Laxfordian fold axial trace across the fault trace on Barra. The presence of Torridon Group sediments in the Minch and Sea of the Hebrides Basins (i.e., in the hanging wall to the OHFZ; Figure 2b) suggests, however, that the magnitude of Caledonian thrusting in the Outer Hebrides must have been small and implies that the lower end of this range may be more appropriate. Assuming maximum updip displacements of between 2 and 3 km and a fault dip of 30°, the thrust-related increase in crustal thickness would have been ~1-2 km. The thermal and rheological implications of crustal thickening are discussed in section 4.

In the Uists the brittle, thrust-related faults are overprinted in the eastern part of the exposed fault zone by a lower greenschist facies, sinistral strike-slip-related fabric (Figure 2a). The intensity of this macroscopically ductile fabric is heterogeneous, producing a braided network of NNE to NE trending phyllonitic shear zones in eastern North Uist [*White and Glasser*, 1987; *Imber et al.*, 1997] (Figures 4 and 5) and a single, N-S trending phyllonite belt along the east coast of South Uist [*Coward*, 1972; *Butler et al.*, 1995; *Osinski et al.*, 2001] (Figure 2a). Whole-rock K-Ar ages obtained from phyllonites in the Uists cluster around 400 Ma (D. C. Rex as discussed by *Sibson* [1977b]), implying a Late Caledonian age for phyllonitization and greenschist facies metamorphism along the southern segment of the OHFZ [*Butler et al.*, 1995]. Indirect displacement estimates based on comparing (1) magnetic intensities and susceptibilities [*Piper*, 1992] and (2) the trends of Proterozoic dykes [*Lisle*, 1993] in the Outer Hebrides to the west of the OHFZ with those associated with the Lewisian Complex on the Scottish mainland (Figure 2a, inset) suggest that the Outer Hebrides have been displaced by 85-95

km in a sinistral sense relative to mainland Scotland. The unequivocal kinematic evidence for sinistral strike slip preserved onshore in the Outer Hebrides (section 3) suggests that these displacements were accommodated by slip along the OHFZ (see *Butler et al.* [1995] and *MacInnes et al.* [2000] for discussion). Strike slip was followed by top to the east or SE extension accommodated by brittle faulting, reactivation of the preexisting phyllonitic shear zones, and the development of a "new" greenschist facies phyllonitic fabric (section 3). Analysis of primary, two-phase fluid inclusions trapped in a syntectonic quartz vein constrains the temperature of extension-related phyllonitization to 370° ± 20°C [*Osinski et al.*, 2001] (Figure 3a). On South Uist, the OHFZ is locally cut by undeformed quartz-diorite and camptonite dykes whose intrusion age is dated between 304 and 280 Ma (Rb-Sr biotite ages [*Fettes et al.*, 1992]) (Figure 3a). This observation shows that most onshore movement in the Uists must predate the Permo-Carboniferous. Thus the final phase of top to the east/NE brittle deformation observed onshore along the southern segment is likely to be of Carboniferous age or older and was probably controlled by faulting along the western margin of the Sea of the Hebrides Basin (Figure 2b).

Interpretations of combined outcrop, seismic, borehole, and published geochronological data show that the Outer Hebrides Fault Zone is a crustal-scale structure that was active for at least 1000 Myr (Table 1). The heterogeneous fault rock assemblage implies a complex thermal and rheological history that was associated with at least three separate phases of greenschist facies metamorphism and phyllonitization. There is an overall asymmetry to the fault rock distribution, with phyllonitic fabrics restricted to the eastern parts of the exposed fault zone (i.e. toward the hanging wall) and brittle, thrust-related fault rocks cropping out toward the west (i.e., toward the footwall; e.g., Figures 2b and 4). *Sibson* [1977a, 1977b] argued that the observed change from brittle faulting in the west to macroscopically ductile deformation in the east reflected a mainly temperature-controlled transition from frictional behavior to quasi-plastic (i.e., viscous) flow during top to the NW thrusting. This interpretation requires that the brittle and macroscopically ductile deformation events formed more or less contemporaneously during a single, progressive kinematic event. Thus the present-day erosion surface was thought to preserve an asymmetrically exhumed depth section through the frictional-viscous transition zone of a crustal-scale, top to the west Caledonian thrust zone, with an eastward increase in paleotemperature (see *Sibson* [1977a, figure 1]). Our observations, together with those of previous studies [*White and Glasser*, 1987; *Butler et al.*, 1995; *Imber et al.*, 1997], however, cast doubt on *Sibson's* [1977a, 1977b] interpretation as they demonstrate that the phyllonitic fabrics are kinematically distinct and consistently overprint the brittle, thrust-related structures.

3. Geological Evidence for Frictional and Viscous Deformation Along the OHFZ

3.1. Outline

Sections 3.2. and 3.3. provide detailed field and microstructural descriptions of (1) the Caledonian-age phyllonites and their precursor fault rocks from North and South Uist (section 3.2.) and (2) the Proterozoic- and Caledonian-age phyllonites from Scalpay (section 3.3.). These localities are, respectively, broadly representative of the fault rocks exposed throughout the southern and northern fault zone segments (Figure 2a). We deal first with the southern segment of the OHFZ in North Uist as it was used by *Sibson* [1977a] as his type section. The relative ages of the fault rocks are established, then the geological data are interpreted in terms of the prevailing kinematic regime, metamorphic environment, and operative deformation mechanisms at the time of fault rock formation along each segment of the OHFZ. The principal findings are summarized in section 3.4., and the implications of our results for the nature of frictional-viscous transition are discussed in section 4.

3.2. Caledonian Deformation and Phyllonitization Along the Southern Segment

3.2.1. Distribution and relative ages of fault rocks, North Uist. The examples discussed here are mainly from the well-exposed Burrival–Eigneig Bheag region but are representative of Caledonian-age structures preserved throughout eastern North Uist (for more detailed accounts, see *Butler* [1995] and *Imber* [1998]) (Figures 4 and 5). The protolith assemblage consists of quartzo-feldspathic banded gneisses, associated with large (< 100 m diameter) metabasite pods and occasional pegmatite sheets [*Fettes et al.*, 1992]. Thrust-related deformation is extremely heterogeneous and is characterized by a thick (> 1 km), east dipping belt of "crush melange", associated with a number of high-strain, NNE-SSW striking "pseudotachylyte-ultracataclasite crush zones" [*Sibson*, 1977a, 1977b; *White and Glasser*, 1987]. The crush melange comprises variably fractured blocks of parent gneiss, ranging from a few centimeters up to 100 m in diameter, crosscut by multiple generations of predominantly NNE-SSW trending cataclasite- and/or pseudotachylyte-bearing faults and injection veins (Figure 5, stereonets a and b, and Figure 6a). The crush zones (< 30 m thick) are characterized by a few, randomly oriented clasts of brecciated gneiss (typically < 1 m in diameter), which "float" in an ultrafine-grained, intensely fractured matrix of ultracataclasite and devitrified pseudotachylyte (matrix ≤ 70% by volume). Kinematic indicators are rarely preserved, although *Butler* [1995] noted that the geometries of pseudotachylyte-bearing faults developed in regions adjacent to the crush zones generally indicate top to the west overthrusting [cf. *White and Glasser*, 1987].

To the east of Loch a' Ghlinne-dorcha the brittle fault rocks are overprinted by a pervasive, low-strain protophyllonitic fabric that locally intensifies to produce an interconnected network of high strain, phyllonitic shear zones (Figure 5). While the high-strain shear zone fabrics clearly accommodated most of the deformation, the incipient, low-strain fabrics preserve important information relating to the early development of these macroscopically ductile phyllonites and thus hold the key to understanding the phyllonitization process along the OHFZ. The crude, protophyllonitic foliation dips to the SE or NW (Figure 4, stereonets b(i) and c(i)) and, at the outcrop scale, is defined by sheared cataclasite/pseudotachylyte veins and flattened blocks of felsic and mafic gneiss (Figures 6b and 6c). Thus the ductile protophyllonitic fabric is clearly seen to overprint the brittle fault rocks

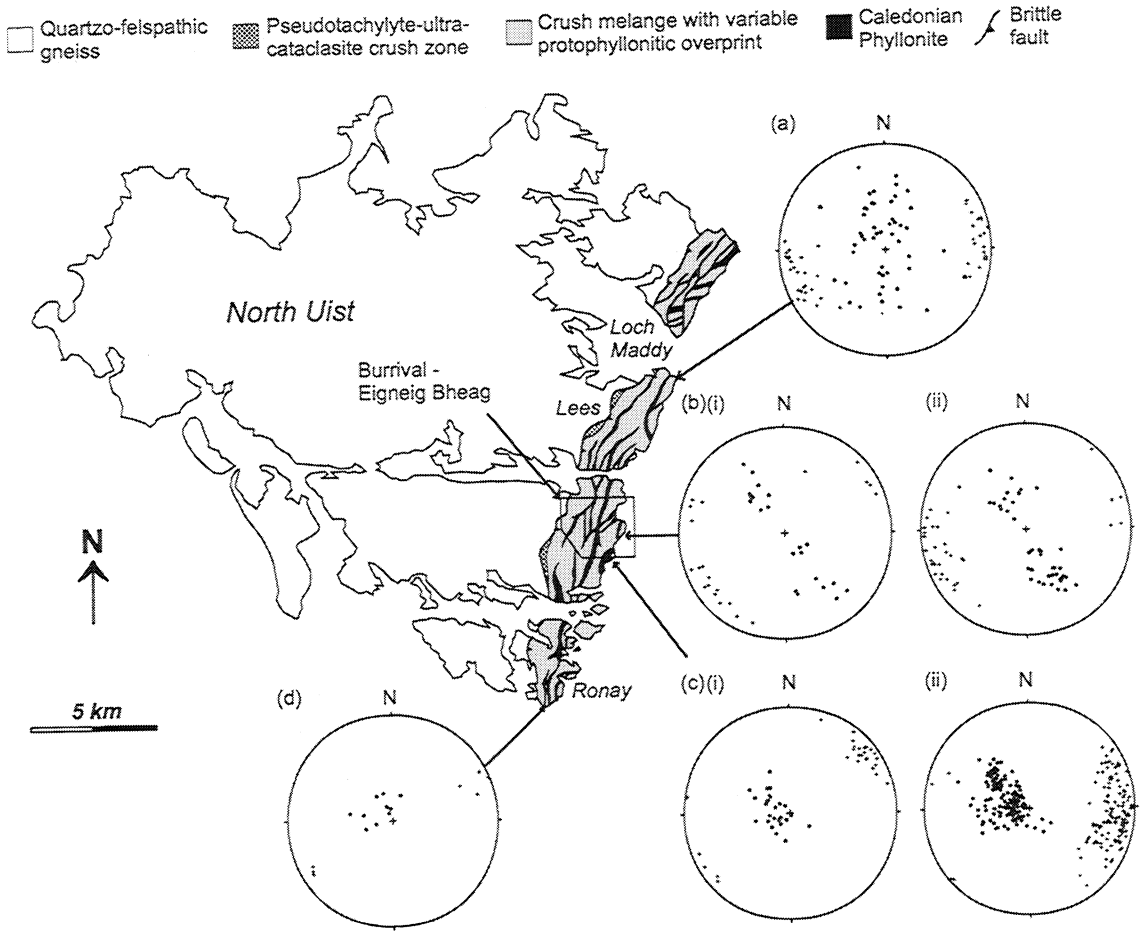

Figure 4. Simplified geological map of the Outer Hebrides Fault Zone showing the distribution of fault rocks in North Uist, complied from *Fettes et al.* [1992], *Butler* [1995], and *Imber* [1998]. Stereonets show the orientations of fabrics in protophyllonitic and phyllonitic rocks (dots are poles to foliation and crosses are mineral stretching lineations). Stereonets are as follows: a, Lees area, phyllonitic fabrics; b, Eigneig Mor area (see Figure 5), protophyllonitic fabrics (stereonet i) and phyllonitic fabrics (stereonet ii); c, Eigneig Bheag area (see Figure 5), protophyllonitic fabrics (stereonet i) and phyllonitic fabrics (stereonet ii); (d) Ronay area, phyllonitic fabrics.

associated with the crush melange. The foliation carries a subhorizontal, NE-SW trending mineral lineation (Figure 4, stereonets b(i) and c(i)) and widespread kinematic indicators (sigmoidal bending of fabrics, asymmetric shear bands, and σ-type quartz porphyroclasts) viewed in surfaces parallel to the lineation but perpendicular to the foliation that are everywhere consistent with top to the NE (sinistral) shear (e.g., the bending of the fabric in Figure 6b). In contrast to *Sibson's* [1977a, 1977b] interpretation, these observations show unequivocally that the macroscopically ductile, sinistral strike-slip-related fabrics overprint, and therefore postdate the brittle, thrust-related rocks of the crush melange. The implications of our revised chronology for the structural and rheological evolution of the OHFZ during Caledonian deformation are discussed in section 3.2.3.

The NNE to NE trending phyllonitic shear zones (Figure 6d) are between 2 and 30 m thick and are characterized by a platy, SE or locally NW dipping foliation that typically strikes clockwise of local shear zone margins (Figure 4, stereonets a(i), b(ii), c(ii), and d). This sense of asymmetry is consistent with sinistral motion across the phyllonitic shear zones (see below). The foliation is defined by aggregates of fine-grained, strongly aligned phyllosilicate minerals, stretched-out quartz-feldspar aggregates and what appear to be reworked, intensely deformed cataclasite and/or pseudotachylyte veins. Subhorizontal, NE-SW trending mineral lineations and associated sinistral shear sense criteria are typically preserved in foliation planes close to shear zone margins, but ENE to SE plunging lineations dominate the central regions (Figure 4, stereonets b(ii) and c(ii)). At well-exposed localities (e.g., NF 920 600, Figure 5), we observed a progressive, clockwise reorientation of the mineral lineation from a strike-parallel, NE-SW orientation along shear zone margins to a downdip, ESE plunging attitude at the centers of individual shear zones. Here the foliation is deformed by asymmetric shear bands and strongly flattened chevron folds (Figure 6e), the geometries of which, when viewed in surfaces parallel to the ESE plunging mineral lineation, are everywhere consistent with top to the ESE (i.e. downdip) shear. Interconnected systems of ESE to SE dipping detachment faults and ESE verging buckle folds

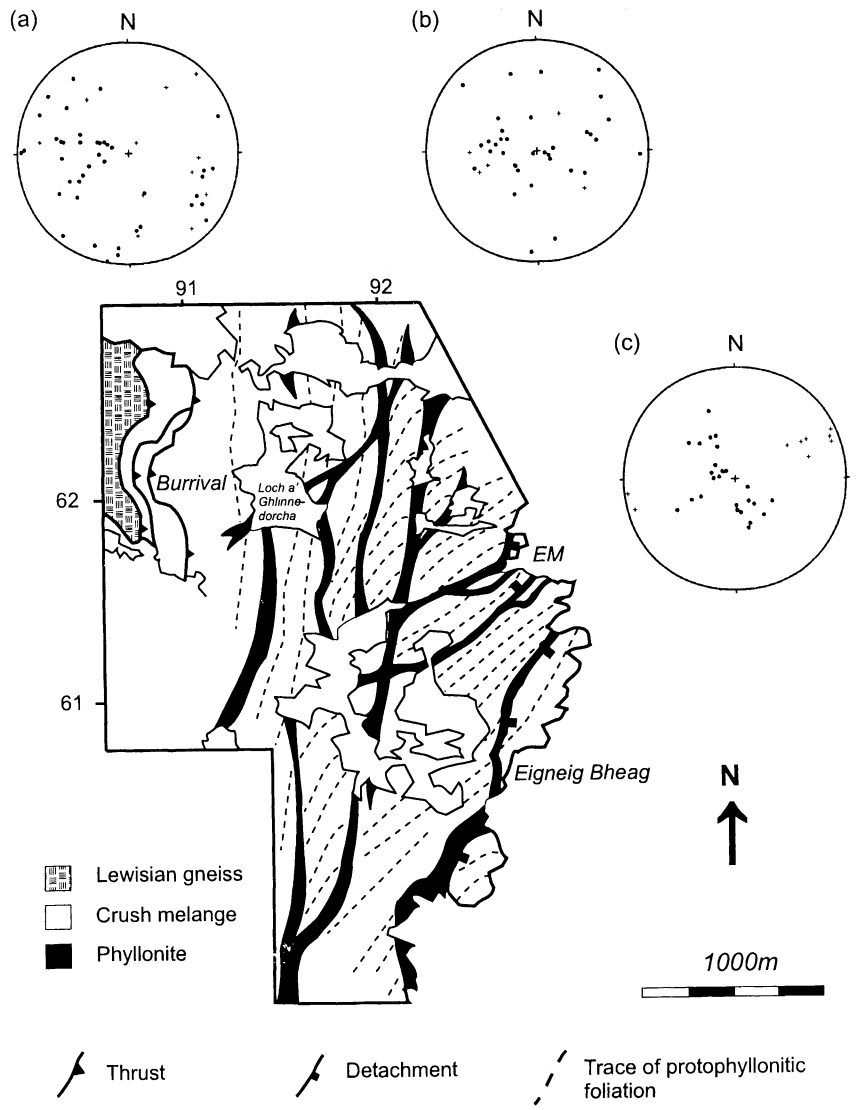

Figure 5. Geological map of the Burrival–Eigneig Bheag region, North Uist, after *Butler et al.* [1995]. EM is Eigneig Mor. Note the sigmoidal "curve-in" of the protophyllonitic foliation toward the margins of phyllonitic shear zones. Stereonets show the following: a, poles to centimeter- to meter-scale brittle faults within the crush melange (dots) and slickenline lineations (crosses); b, poles to cataclasite/pseudotachylyte veins (dots) and slickenlines (crosses) within the crush melange; and c, poles to brittle detachment faults (dots) and slickenline lineations (crosses), Eigneig Bheag–Eigneig Mor region.

are widely developed within and along the margins of extensionally reworked shear zones (Figure 6f). These structures are associated with multiple generations of syntectonic, foliation-parallel, and axial planar quartz-calcite veins that are commonly observed to be sheared out and attenuated parallel to the phyllonitic foliation [*Imber*, 1998]. This suggests that periodic buildups in pore fluid pressures led to cyclic hydraulic fracturing and transient phases of embrittlement during extension-related shear zone reactivation. Brittle, mainly foliation-parallel SE to ESE dipping, pre-Permo-Carboniferous strike slip and normal faults (associated with top to the NE and east shear sense criteria, respectively, Figure 5, stereonet c) carry gouge and are everywhere seen to crosscut all other fabrics and structures [*Imber*, 1998]. They therefore represent the final phase of fault-related deformation preserved onshore on North Uist.

Our observations show that the effects of top to the ESE extension overprint the earlier, sinistral strike-slip-related fabrics and demonstrate that almost all of the extensional movement was accommodated by brittle-ductile deformation within and along the margins of the preexisting phyllonitic shear zone network. The final phase of top to the NE strike slip involves entirely brittle deformation of the fault zone and suggests that by the close of Caledonian deformation the present-day erosion level lay within a few kilometres (less than ~5 km) of the paleosurface [cf. *Lewis et al.*, 1992].

3.2.2. Distribution and relative ages of fault rocks, South Uist. On South Uist the brittle, basal thrust of the

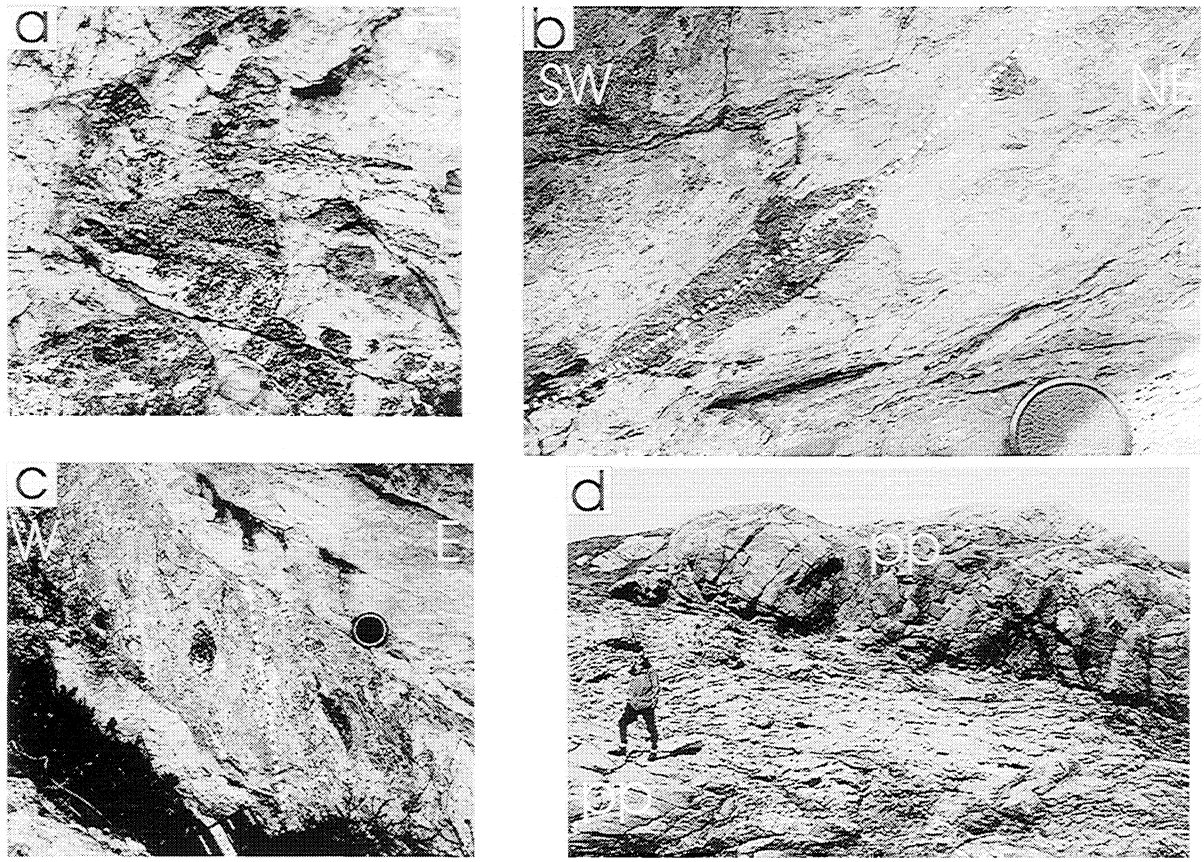

Figure 6. Fault rocks from the OHFZ in North and South Uist. (a) Randomly oriented blocks of fractured gneiss floating in pale ultrafine-grained cataclasite matrix typical of the crush melange, Burrival, North Uist (NF 908 619). (b) Flattened clasts of mafic (dark) and acid (light) gneiss surrounded by cataclasite matrix (medium gray) of crush melange all overprinted by moderately east-dipping protophyllonitic fabric (dashed line), Burrival, North Uist (NF 909 620). (c) Flattened clasts of gneiss surrounded by cataclasite matrix of crush melange overprinted by steeply east-dipping protophyllonitic fabric (dashed line) and later, moderately east-dipping brittle faults, Burrival, North Uist (NF 909 619). (d) Well-exposed ESE dipping phyllonitic shear zone (obviously foliated rocks) cutting protophyllonitic crush melange (more massive rocks labeled pp), Eigneag Bheag, North Uist (NF 921 596). (e) Top to ESE verging chevron folds (highlighted with dashed lines, top part of exposure) and top to the ESE shear bands (arrowed, herringbone ribs below lens cap) from phyllonitic shear zone shown in Figure 6d, Eigneag Bheag, North Uist (NF 921 596). (f) Updip view of downdip, ESE verging folds and top to the E, anastomosing detachment faults (half arrows), Eigneag Bheag, North Uist (NF 921 597). (g) Deformed Laxfordian pegmatite in mylonites with top to the NW S-C fabrics, exposure at the margins of the Lag na Laire low-strain zone, Scalpay (NG 231 942). (h) Downdip, lineation-parallel view of phyllonite showing top to NE (sinistral) shear bands in Caledonian phyllonite. Quarry exposures, Cnoc na Croich shear zone, Scalpay (NG 224 957).

OHFZ has emplaced a late Archaean, granulite facies pyroxene metagabbro body ("Corodale Gneiss" [*Coward*, 1972; *Whitehouse*, 1993; cf. *Osinski et al.*, 2001]) over amphibolite facies Lewisian gneisses in its footwall (Figure 7, stereonet a). The Corodale Gneiss forms a relatively intact unit that contrasts strongly with the wide belt of crush melange seen in North Uist. The upper margin of the Corodale Gneiss is defined by a single, east dipping phyllonitic shear zone ("Usinish Phyllonite" [*Coward*, 1972; *Butler*, 1995]) that carries a unit of intensely deformed, thrust-related quartzo-feldspathic crush melange ("Mashed Gneiss" [*Coward*, 1972; *Butler*, 1995]) in its hanging wall (Figure 7).

The Usinish Phyllonite and its margins are best exposed at Rubha Bolum (NF 830 284) where we have mapped four distinct, fault-bounded packages of phyllonite and protophyllonite (Figures 7 and 8). Domains 3 and 4 are the structurally highest units comprising two panels of intensely sheared, north dipping phyllonite derived from Corodale Gneiss and a low-strain "pod" of weakly phyllonitised (i.e. protophyllonitic) Mashed Gneiss, respectively. Both units carry subhorizontal NE-SW mineral lineations (Figure 8, stereonets c and d) that are associated with abundant top to the NE (sinistral) shear criteria. These observations demonstrate that the low-strain, strike slip fabrics that are exposed in domain 4 over-

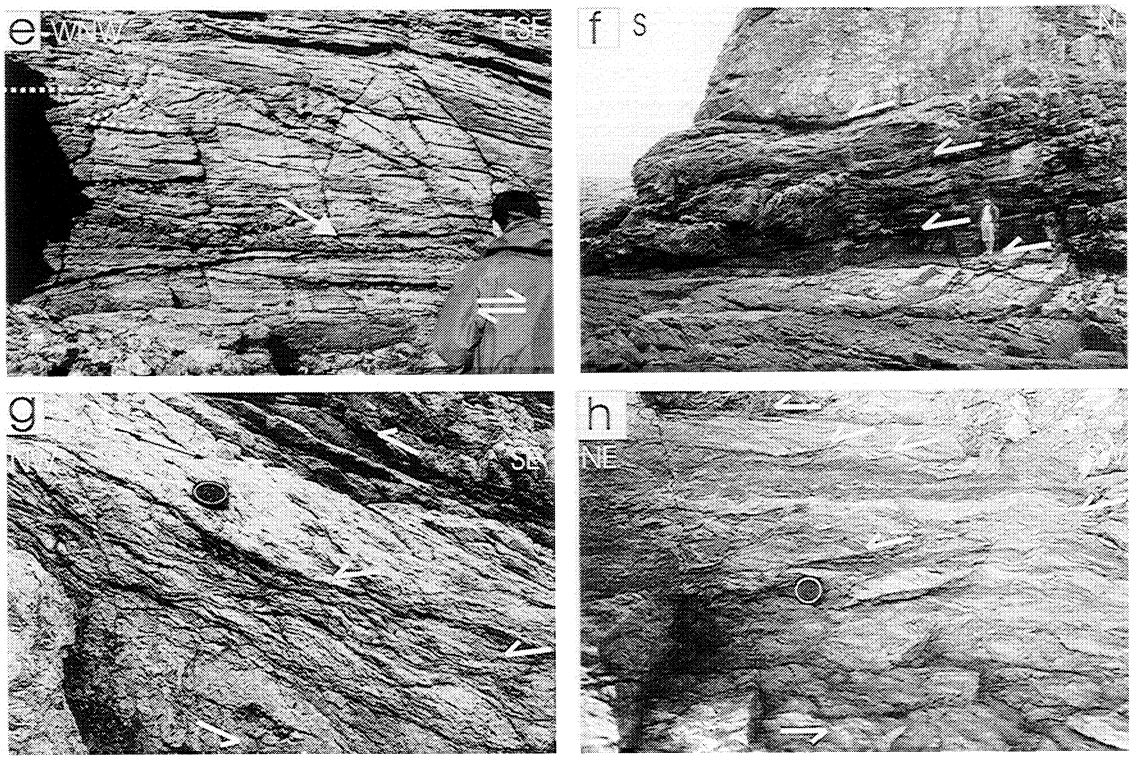

Figure 6. (continued)

print and therefore postdate the products of brittle, thrust-related deformation in the Mashed Gneiss. We infer, based on the structural relationships observed in domain 1 (see below), that the high-strain, Corodale Gneiss-derived phyllonites preserved in domain 3 also developed during sinistral strike slip (see also Figure 7, stereonet b). The base of the Usinish Phyllonite is exposed in domains 1 and 2. Here the original shear zone margin is preserved as a gradational contact between intensely fractured Corodale Gneiss in the west and an eastward intensifying but generally low-strain, protophyllonitic fabric to the east. The east to SE dipping foliation is, in both domains, defined by aggregates of aligned phyllosilicate minerals and sheared cataclasite- or pseudotachylyte-bearing fault veins. In domain 1 the foliation is associated with a subhorizontal, NE-SW trending mineral lineation, while in domain 2, it carries an east plunging, downdip mineral lineation (Figure 8, stereonets a and b). Kinematic indicators (δ-type quartz porphyroclasts) viewed in surfaces parallel to these lineations are consistent with top to the NE (sinistral strike slip) and top to the east (downdip extensional) shear in domains 1 and 2, respectively. The overprinting relationships once more show that the phyllonitic fabrics postdate the effects of brittle, thrust-related deformation. In domain 2, however, phyllonitization appears to have been synchronous with top to the east extension. Thus we have evidence for two phyllonitization events at Rubha Bolum. On the basis of the kinematic history deduced along strike in North Uist we suggest that the sinistral strike-slip fabrics are the earlier event while the top to the east extension is later. Our observations are in good agreement with those of *Osinski et al.* [2001], who describe evidence for extension-related phyllonitization within the Usinish Phyllonite at localities to the south of Rubha Bolum. The domain bounding faults at the latter locality are gently east dipping detachments carrying narrow bands of soft, clay-rich gouge that probably developed during late, near-surface deformation (see section 3.2.1.). Associated slickenlines plunge ENE (Figure 7, stereonet c), and second-order Riedel fracture patterns suggest that the detachments developed during top to the ENE displacements.

To summarize, detailed structural mapping along the southern segment of the OHFZ shows that the macroscopically ductile phyllonites and protophyllonites everywhere postdate the effects of brittle, thrust-related deformation. We have identified two phases of Caledonian phyllonitization; the first occurred during sinistral strike slip, and the second was synchronous with later top to the east extension. Extensional deformation was accommodated by brittle-ductile reactivation of the preexisting shear zones and, less commonly, by generation of new phyllonitic fabrics along shear zone margins (as seen only on South Uist). The last phase of brittle, top to the NE or ENE strike slip/extension occurred near the paleosurface and records the final, post-Caledonian (?) embrittlement of the fault zone.

3.2.3. Microstructure and deformation environment.

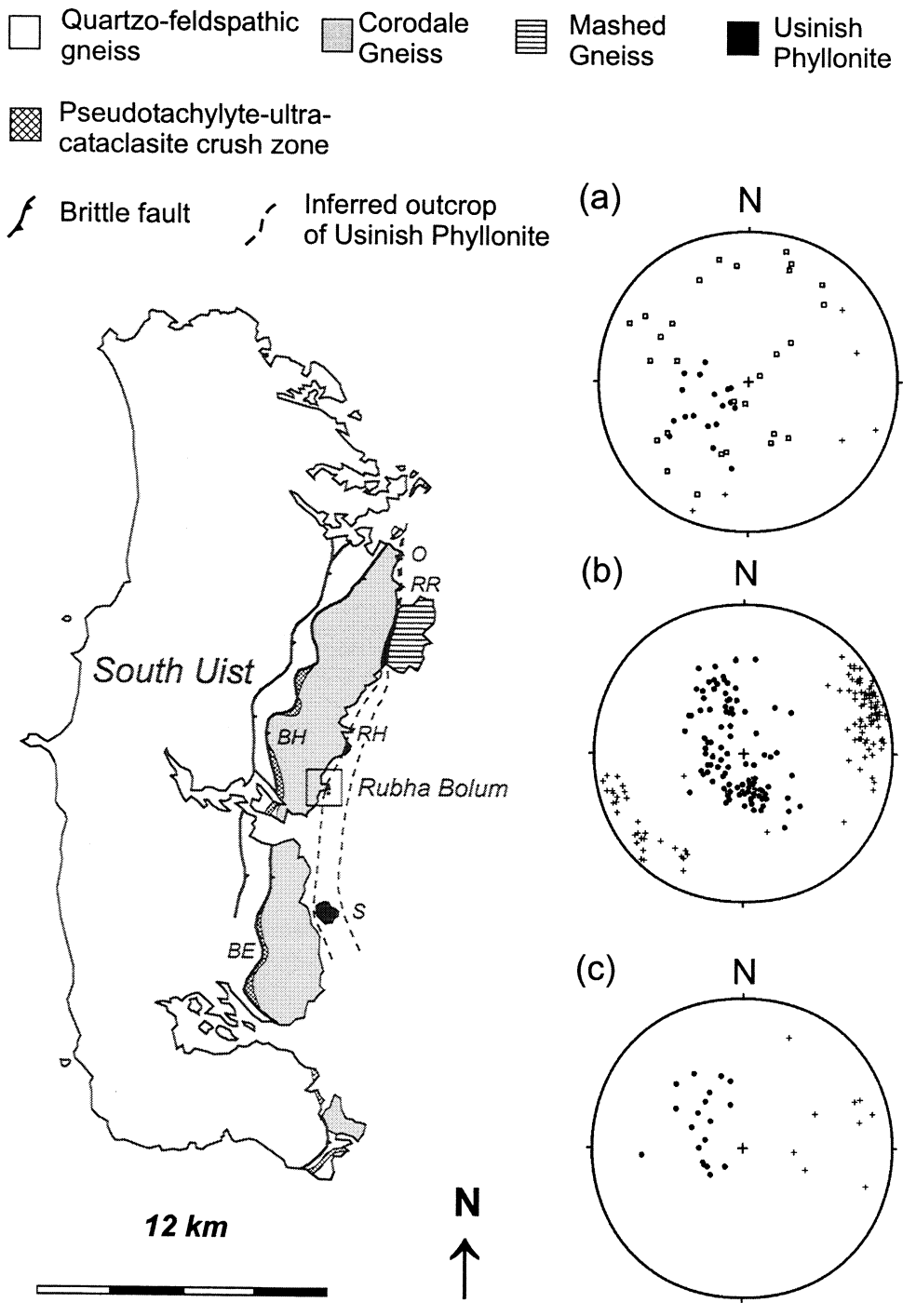

Figure 7. Simplified geological map of the Outer Hebrides Fault Zone showing the distribution of fault rocks in South Uist. Stereonets show the following: a, poles to brittle faults (dots) and cataclasite/pseudotachylyte-bearing fault veins (squares) and slickenline lineations (crosses) (data collected from Ben na Hoe (BH), Bealach an Easain (BE) and Rubha Rossel (RR)); b, phyllonitic fabric elements associated with the Usinish Phyllonite, dots are poles to foliation, crosses are mineral stretching lineations (data collected from Ornish (O), Rubha Rossel (RR), Rubha Hellisdale (RH), Rubha Bolum, and Stuley island (S)); c, poles to brittle detachment faults (dots) and slickenline lineations (crosses) (data collected from Bealach an Easain (BE) and Rubha Bolum).

The evolution in texture and mineralogy of the fault rocks is similar throughout North and South Uist [*Imber*, 1998]. Here we confine our microstructural descriptions to fault rocks from North Uist, alluding to differences with South Uist where they arise. The protolith gneisses comprise interlocking aggregates of equigranular plagioclase (An < 30%), K-feldspar, or hornblende grains (< 1 mm diameter), which enclose pockets of flattened, undulose quartz (< 6 mm long),

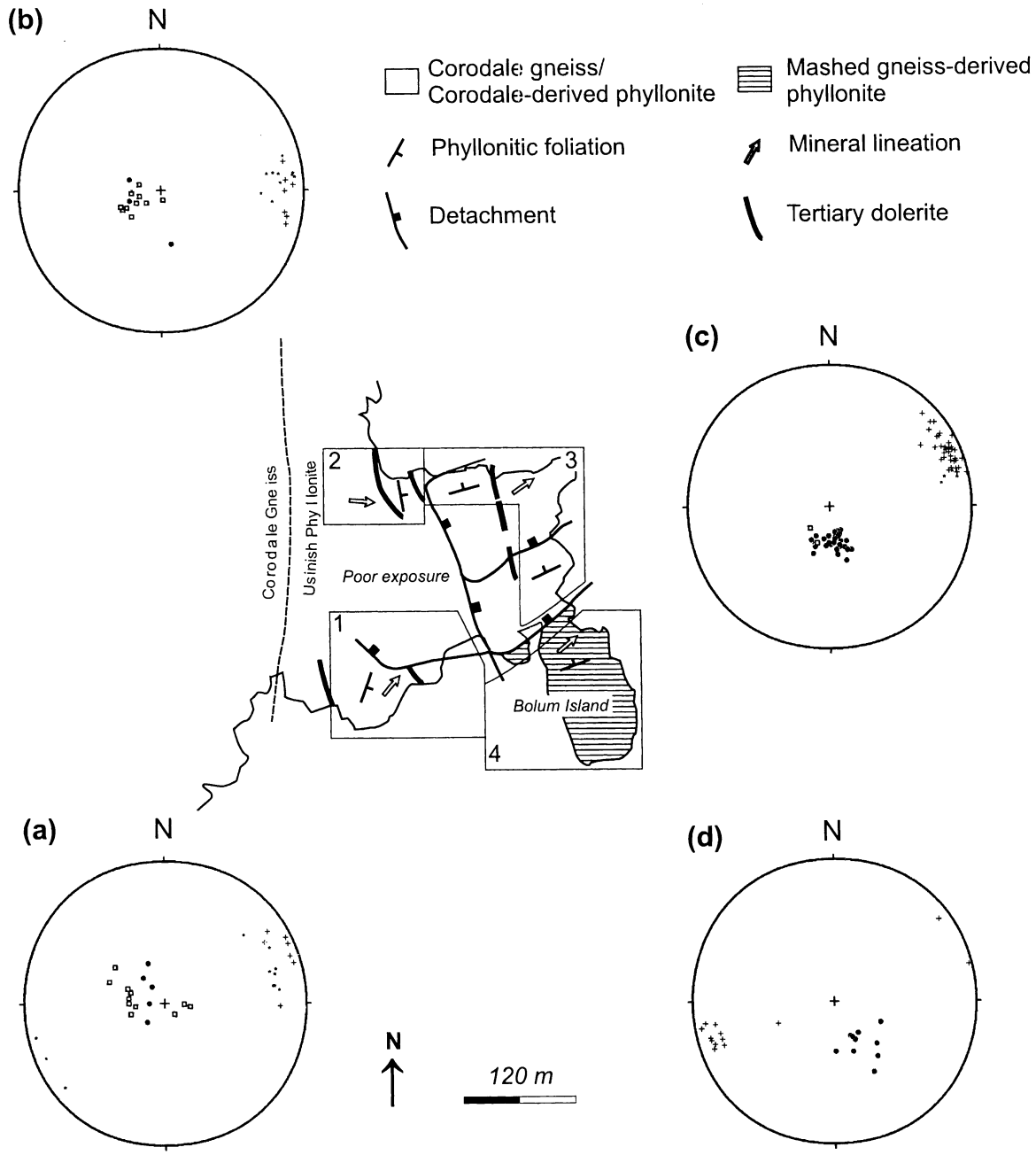

Figure 8. Geological map of the Usinish Phyllonite at Rubha Bolum, South Uist. Boxes 1-4 refer to structural domains discussed in the text. In the stereonets a-c (for domains 1-3, respectively), dots and squares are poles to phyllonitic and protophyllonitic foliation respectively, while in stereonet d (domain 4), dots are poles to protophyllonitic foliation. In all domains, crosses are mineral stretching lineations.

laths of biotite, and epidote grains. Corodale Gneiss and Corodale Gneiss-derived fault rocks have significantly lower quartz and correspondingly higher feldspar contents compared to the quartzo-feldspathic Lewisian gneisses.

Clasts of gneiss preserved within the thrust-related crush melange are crosscut by randomly oriented arrays of transgranular and intragranular shear fractures, cataclasite seams, and devitrified pseudotachylyte veins (Figure 9a). In terms of deformation microstructures, there are no significant differences between the cataclasites and devitrified pseudotachylytes [*Walker*, 1990; *Imber*, 1998], which both consist of angular to rounded clasts of fractured quartz and feldspar dispersed in an ultrafine-grained, isotropic matrix of quartz, albite, and sericite (individual matrix grains << 0.005 mm in diameter). Quartz grains display strong, patchy undulose extinction, with little evidence for recovery or recrystallization. These observations show that deformation in the crush melange was accommodated by brittle fracturing accompanied by limited, low-temperature plasticity in quartz grains [*Lloyd and Knipe*, 1992]. This interpretation implies that the crush

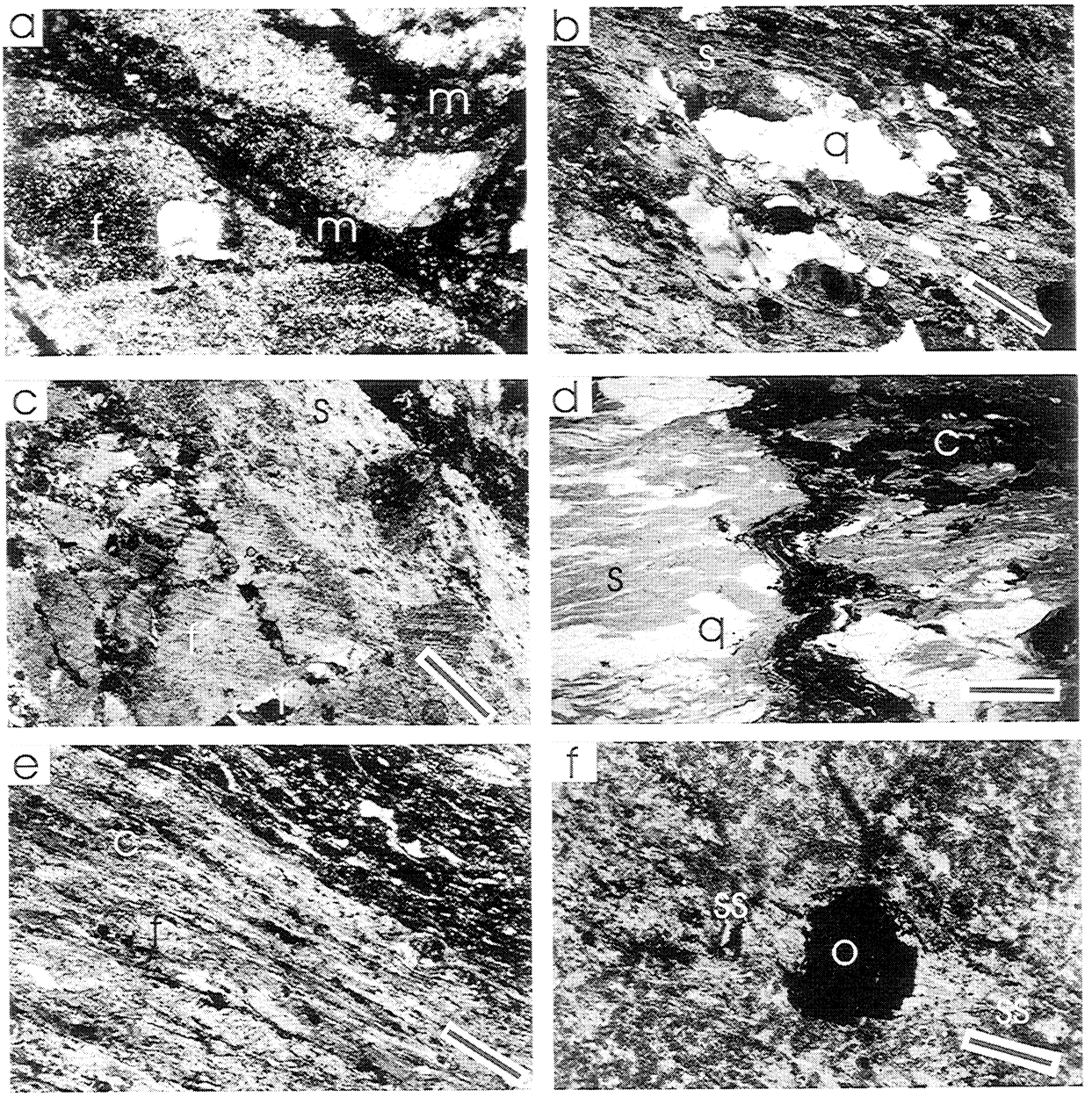

Figure 9. Photomicrographs of fault rocks, North Uist. (a) Cataclasite seam (dark band oriented at ~45° to the long axis of photomicrograph) crosscutting banded gneiss host rocks. Matrix (m) comprises aggregates of ultrafine-grained quartz, feldspar, hornblende, and opaque minerals. Note that feldspar grains (f) preserved in the host rock have suffered partial alteration to fine grained sericite (speckles). This alteration is entirely posttectonic in origin (see text). Field of view is 1.3 × 0.77 mm, with crossed polars. (b) Protophyllonite. Note relatively undeformed quartz porphyroclasts (q) that are locally wrapped by strands of sericite (s), derived from the chemical breakdown of feldspar (see text for discussion). Bar lies parallel to mineral lineation. Field of view is 3 × 1.9 mm, with crossed polars. (c) Partially altered feldspar grain in protophyllonite. Relatively unaltered region (f) is crosscut by intragranular extension fractures (e.g. t). Highly sericitised margins (s) begin to deform in a macroscopically ductile manner as the sericite needles become aligned parallel to the foliation. Bar lies parallel to trace of foliation. Field of view is 1.3 × 0.77 mm, with crossed polars. (d) Protophyllonite. Collapse of the interlocking network of feldspar grains (s) and the development of a penetrative, sericite-rich protophyllonitic foliation (parallel to bar) lead to collapse and flattening of the entire rock, as highlighted by folding of relict cataclasite seams (c) and relatively undeformed quartz porphyroclasts (q). Field of view is 13.5 × 8 mm, with plane polarized light. (e) Phyllonite. Partially altered feldspar grains (f) wrapped by network of interconnected chlorite strands (c). Dark, well-foliated material (top right) is derived from highly altered and deformed cataclasite or pseudotachylyte. Bar parallel to mineral lineation. Field of view is 3×1.9 mm, with plane polarized light. (f) Opaque grain (o) preserved in epidote-rich phyllonite fringed by quartz-chlorite strain shadows (ss). The matrix comprises highly altered and deformed cataclasite or pseudotachylyte. Bar is parallel to mineral lineation. Field of view 1.3 × 0.77 mm, with plane polarized light.

melange developed at temperatures of less than ~250°–300°C (the range of temperatures above which quartz undergoes widespread, crystal plastic deformation) and shows that thrusting occurred entirely within the frictional flow regime as defined by *Schmid and Handy* [1991]. Thus, the present-day erosion surface must have been above the level of the paleo-frictional-viscous transition during Caledonian thrusting. Despite widespread evidence for static, posttectonic retrogression within the crush melange [*Walker*, 1990; *Imber*, 1998] (Figure 9a) the frequent occurrence of pseudotachylyte and the lack of microstructural evidence for syntectonic fluid-rock interaction [e.g., *Knipe*, 1989] strongly suggest that thrusting occurred in a "dry", fluid-absent environment.

Both strike-slip and extension-related phyllonites comprise fine-grained aggregates of feldspar, sericite, chlorite, actinolite, epidote, opaque minerals, and on North Uist, quartz and calcite. Protophyllonites contain a high proportion of fractured gneiss-derived material, while shear zone-related phyllonites largely consist of ultrafine-grained material derived mainly from reworked cataclasite and pseudotachylyte veins. On a microscopic-scale the foliation in material derived from fractured gneiss is defined by aggregates of aligned sericite grains and trails of ultrafine-grained albite ± epidote (individual albite grains < 0.02 mm diameter) (Figure 9b). Thin section observations indicate that these minerals were derived from the chemical alteration of plagioclase and K-feldspar grains in the parent gneiss, according to reactions such as

$$20 \text{ oligoclase} + 2 \text{ K-feldspar} + 3H_2O + Fe_2O_3 \rightarrow 2 \text{ sericite} + 16 \text{ albite} + 2 \text{ epidote} + 2SiO_2 \quad (1)$$

[*Pryer and Robin*, 1995]. The early stages of feldspar alteration are characterized by the appearance of small, randomly oriented sericite flakes within the host grain and irregular patches of ultrafine grained albite ± epidote along grain margins. Relatively unaltered feldspar grains (sericite < 20% by volume) are crosscut by arrays of intragranular extension fractures infilled by calcite, epidote, and/or fibrous quartz-chlorite-actinolite intergrowths (Figure 9c). Progressive alteration is marked by an increase in the volume of sericite and albite at the expense of the parent grain and a decrease in the number of intragranular fractures. Albite-rich aggregates become "strung out" parallel to the macroscopic foliation, and at ~20% by volume phyllosilicate, individual sericite needles appear to coalesce to form a continuous, anastomozing network of sericite-rich foliae [*Imber et al.*, 1997]. The breakdown of individual feldspar grains leads to the eventual collapse of the interlocking network of feldspar grains in the fractured gneiss to produce a well-defined protophyllonitic fabric (Figures 9c and 9d). Quartz porphyroclasts display strong, patchy undulose extinction (Figure 9b) and are commonly observed to be crosscut by intragranular extension fractures infilled by fibrous, quartz-chlorite-actinolite (± calcite) aggregates. On North Uist, deformed calcite grains display well-developed undulose extinction and are characterized by type 3 deformation twins, implying that deformation and phyllonitization occurred at temperatures of > 200°C [*Burkhard*, 1993]. Hornblende is almost entirely replaced by aggregates of chlorite ± actinolite and breaks down according to reactions such as

$$3 \text{ amphibole} + 2 \text{ epidote} + 10CO_2 + 8H_2O \rightarrow 3 \text{ chlorite} + 10 \text{ calcite} + 21SiO_2 \quad (2)$$

[*Skelton et al.*, 1995]. Microstructural observations of the low-strain fabrics show that phyllonitization produced a syntectonic mineral assemblage sericite, quartz, albite, actinolite, chlorite, epidote, and calcite. Ca-plagioclase and hornblende appear to have been unstable and were replaced by albite + epidote and chlorite +/- actinolite, respectively. The presence of calcite indicates that the chemical activity of CO_2 was high, at least locally, during phyllonitization [*Yardley*, 1989]. Thus, taking account of (1) the relatively restricted chemical compositions of the parent gneisses, and (2) the presence of CO_2 during deformation, comparison with mineral assemblages developed in regionally metamorphosed basic rocks [*Miyashiro*, 1994] suggests that strike-slip- and extension-related phyllonitization probably occurred under prehenite-pumpellyite to greenschist facies conditions at temperatures of between 250° and 400°C [*Yardley*, 1989]. This range is broadly consistent with a homogenization temperature of 370° ± 20°C obtained from fluid inclusions in an extension-related quartz vein [*Osinski et al.*, 2001] (section 2), and we suggest that phyllonitization probably occurred at temperatures of ~350°C.

Intensely deformed, shear zone-related phyllonites are characterized by isolated quartz, highly altered feldspar, and occasional opaque porphyroclasts dispersed in a contiguous, ultrafine-grained quartz-albite-sericite-epidote-chlorite-opaque matrix (individual grains <<0.01 mm diameter) (Figure 9e). In contrast to quartz grains preserved in the lower-strain protophyllonites, the quartz porphyroclasts typically show well-developed core-and-mantle microstructures and are locally flattened parallel to the phyllonitic foliation. Almost all the porphyroclasts are "wrapped" by fibrous quartz-chlorite strain shadows that are oriented parallel to the macroscopic mineral lineation (Figure 9f). On a microscopic-scale the platy foliation is defined by aligned sericite and chlorite grains, trails of albite/recrystallized quartz, a well-developed pressure solution cleavage, and boudinaged quartz-epidote-calcite veins. Following the arguments of *Jordan* [1987] and *Handy* [1990], we interpret the bulk rheological properties of the shear zone-related phyllonites as having been controlled by the deformation response of the ultrafine-grained, cataclasite- or pseudotachylyte-derived matrix and the contiguous, phyllosilicate-rich foliae. The fine grain size prevents direct (optical) study of the matrix, but the widespread occurrence of pressure solution seams, deformed veins, and fibrous, syntectonic overgrowths and fracture infills strongly suggest the operation of grainsize-sensitive, fluid-assisted diffusive mass transfer mechanisms [*Knipe*, 1989; *McCaig and Knipe*, 1990]. Previous studies suggest that pressure solution and fluid-assisted mass transfer processes are likely to have been important during the development of the phyllosilicate-rich foliae [*Hippertt*, 1994a]. However, the morphology and strong preferred orientation of sericite grains within the foliation planes implies that these minerals were ideally oriented for pressure-insensitive, intracrystalline basal slip [*Mares and Kronenberg*, 1993; *Goodwin and Wenk*, 1995]; thus we cannot rule out the possibility that crystal-plastic deformation mechanisms also contributed to the development of the sericitic foliation.

Our microstructural observations suggest therefore that phyllonitization was associated with the onset of temperature-sensitive, viscous flow controlled by a combination of fluid-assisted, grain size-sensitive, and crystal-plastic deformation mechanisms. We infer therefore that Late Caledonian sinistral strike slip along the southern segment of the OHFZ was accommodated by heterogeneous viscous flow (as defined by *Schmid and Handy* [1991]), with the deformation focused mainly within the network of phyllonitic shear zones. This interpretation implies that the present-day erosion surface must have been below the level of the Caledonian frictional-viscous transition soon after the establishment of sinistral strike slip.

To summarize, our interpretations of combined field and microstructural data for the southern segment show that the brittle and macroscopically ductile fault rocks preserve evidence for a temporal change from frictional deformation during earlier Caledonian thrusting to viscous flow during later Caledonian sinistral strike slip. Thus the present-day outcrop pattern does not represent an asymmetrically exhumed depth section formed during a single kinematic event, as required by *Sibson's* [1977a, 1977b] model. The observed switch in deformation regime [*Schmid and Handy*, 1991] appears to have been triggered by the onset of fluid-assisted, grain size-sensitive deformation plus or minus fluid-present crystal plasticity synchronous with widespread greenschist facies retrogression and phyllonitization; it does not necessarily reflect an eastward increase in paleotemperature [cf. *Sibson*, 1977a, Figure 1]. We conclude that phyllonitization was a response to the influx of aqueous fluids [*White and Glasser*, 1987; *Imber*, 1998] into the previously "dry" fault zone at the onset of sinistral strike slip. The close association between highly deformed, reworked brittle fault rocks and the phyllonitic shear zone fabrics strongly suggests that the fluids entered the fault zone through the preexisting fault and fracture network [*Imber*, 1998], as proposed by other authors working in faulted basement terrains [e.g., *Tourigny and Tremblay*, 1997; *Guermani and Pennacchioni*, 1998].

3.3. Proterozoic and Caledonian Deformation and Phyllonitization Along the Northern Segment

3.3.1. Distribution and relative ages of fault rocks, Scalpay. The island of Scalpay lies to the north of the South Harris Shear Zones (Figure 2a) and provides the best exposed section, at least 1000 m thick, through a NE-SW trending segment of Proterozoic-age thrust-related shear zone in the northern segment [*Sibson*, 1977b; *Lailey et al.*, 1989; *Butler*, 1995; *Butler et al.*, 1995; *Imber*, 1998] (Figures 2a and 10). In addition, two Caledonian-age phyllonite belts crop out in the SE of the island [*Butler*, 1995; *Butler et al.*, 1995; *Imber*, 1998], providing a useful comparison with the Caledonian-age shear zones exposed along the southern segment. The protolith assemblage on Scalpay consists of quartzo-feldspathic gneisses, metadolerite sheets ("Younger Basics") [*Fettes and Mendum*, 1987] and later Laxfordian pegmatite veins. All intrusive units are postdated by mylonitization (e.g., Figure 6g) and thus provide qualitative indicators of strain within the mylonite belt. Toward the SE of the island they are rotated progressively and increasingly into parallelism with the macroscopically ductile foliation, suggesting an overall increase in strain [*Sibson*, 1977b; *Butler et al.*, 1995]. Three elongate (< 200 m long), macroscopic low-strain zones, in which earlier structures (including Laxfordian-age isoclinal folds) are preserved, occur along the south and west coasts of the island (Lag na Laire, NG 232 942; Eilean Glas, 245 946; and Greinem, 245 955; Figure 10). In these regions of low strain, there is often strong discordance between the metaigneous bodies and the protomylonitic foliation. *Lailey et al.* [1989] suggested that the mylonitic fabric is crosscut by the metadolerite sheets. We are unable to support this proposal. The metadolerites are folded and the protomylonitic foliation forms an axial planar fabric that quite clearly passes through the basic sheets. Furthermore, the same protomylonitic to mylonitic fabric deforms numerous examples of Laxfordian-aged pegmatites (Figure 6g) [*Imber*, 1998]. Thus the mylonitic fabrics are everywhere clearly post-Laxfordian in age.

Outside the macroscopic low-strain zones, the mylonitic fabric consists of interbanded packages (< 5 m thick) of quartzo-feldspathic and phyllosilicate-bearing mylonite (the latter are here termed phyllonitic mylonites to distinguish them from the younger, Caledonian-age phyllonites). Overall, phyllonitic mylonite accounts for < 50% of the total thickness of the mylonite belt and typically occurs in high-strain regions along the SE coast [*Sibson*, 1977b; *Imber*, 1998]. Within packages of quartzo-feldspathic mylonite the SE dipping foliation is associated with a consistently SE plunging quartz stretching lineation (Figure 10, stereonet a), and kinematic indicators (asymmetric shear bands and σ-type quartz and feldspar porphyroclasts; Figure 6g) are everywhere consistent with top to the NW shear (i.e., thrusting) across the mylonite belt. Within packages of phyllonitic mylonite, the SE dipping foliation also carries a NW-SE trending lineation, defined by syntectonic quartz-actinolite or quartz-chlorite fibers (Figure 10, stereonet b). However, in two discrete, highly phyllonitized shear zones (< 5 m thick) which crop out near Cnoc na Croich and Kennavay the lineation has been reoriented into a strike-parallel (i.e., NE-SW) trending attitude (Figure 10, stereonet c) [*Butler et al.*, 1995]. Shear sense criteria (S-C fabrics and σ-type quartz porphyroclasts; Figure 6h) associated with this subhorizontal lineation are consistent with top to the NE (sinistral) deformation within these zones. Similar fault rocks are preserved elsewhere along the northern segment of the OHFZ (e.g., the Park District of SE Lewis) and have been described by Butler *et al.* [1995]. On the basis of their kinematic and textural similarity with the phyllonites of the southern fault zone segment in the Uists, we infer a Caledonian age for these strike slip phyllonites.

To summarize, the field evidence suggests that Proterozoic thrusting was accommodated by macroscopically ductile shear within interlayered packages of quartzo-feldspathic and phyllonitic mylonite. A significant amount of phyllonitization appears to have been synchronous with top to the NW thrusting, and these thrust-related phyllonites are generally associated with regions of higher strain. The thrust-related fault rocks were heterogeneously reworked during subsequent Caledonian, sinistral strike slip along the northern segment of the OHFZ, producing superficially similar phyllonitic fault rocks and structures to those preserved along the southern fault zone segment.

3.3.2. Microstructure and deformation environment. The quartzo-feldspathic Lewisian gneiss protoliths preserved

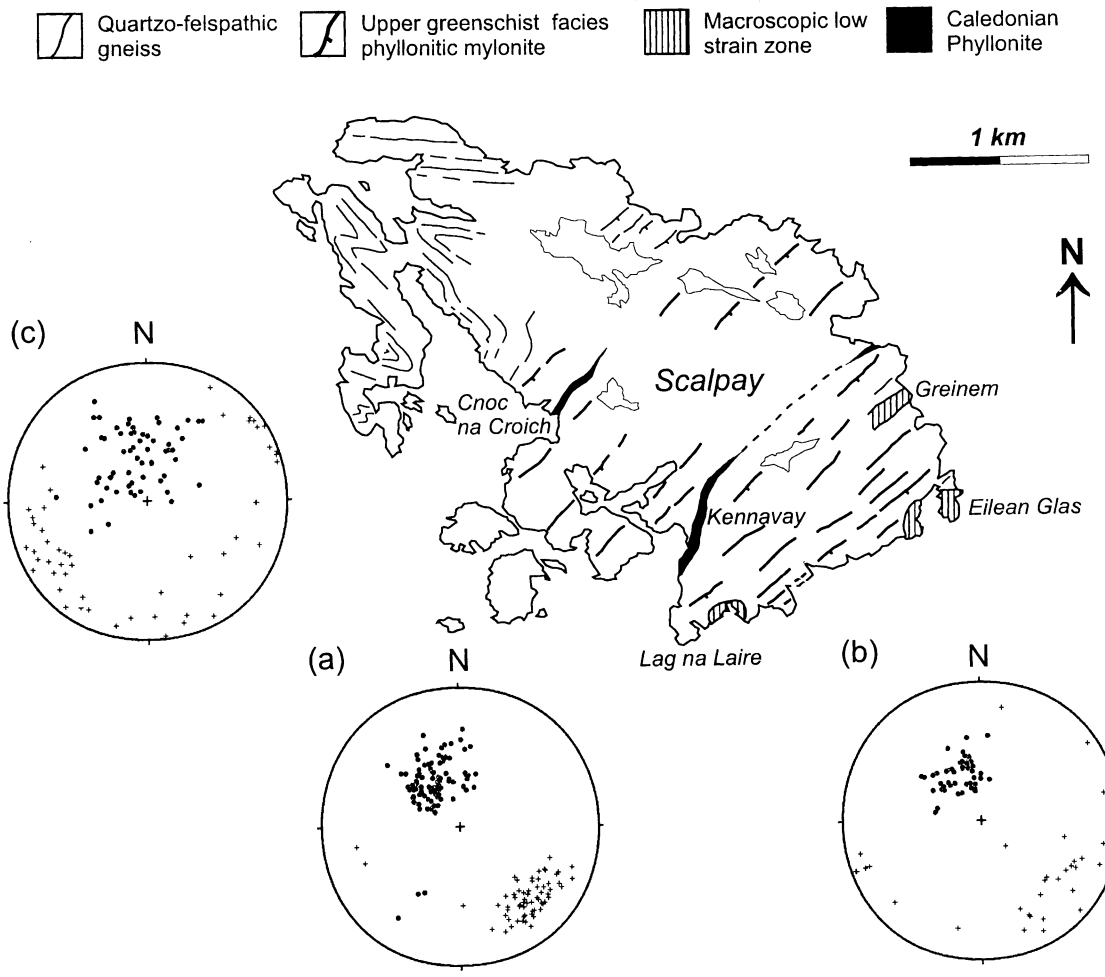

Figure 10. Simplified geological map of the Outer Hebrides Fault Zone showing the fault rock distribution on Scalpay. Map is compiled from *Walker* [1990], *Butler* [1995] and *Imber* [1998]. Stereonets show the following: a, poles to mylonitic foliation (dots) and mineral stretching lineations (crosses), quartzo-feldspathic mylonite; b, poles to foliation (dots) and mineral stretching lineations (crosses), phyllonitic mylonite; c, poles to foliation (dots) and mineral stretching lineations (crosses), Caledonian phyllonite, Cnoc na Croich and Kennavay shear zone.

on Scalpay are microstructurally indistinguishable from those preserved in the Uists (section 3.2.3). The metadolerites comprise equigranular, interlocking hornblende grains (< 2 mm diameter), which enclose pockets of feldspar ± quartz, while pegmatite sheets consist of coarse-grained aggregates of quartz, K-feldspar, and chlorite after biotite (individual grains < 5 cm diameter).

Quartzo-feldspathic mylonite consists mainly of quartz, partially sericitized feldspar (sericite < 5% by volume), hornblende, actinolite, epidote, and less commonly biotite. The foliation is defined by an interconnected network of polycrystalline quartz ribbons (< 0.5 mm thick; aspect ratios < 10:1), which anastomose around isolated feldspar (and hornblende) grains (< 1 mm diameter) (Figure 11a). The quartz ribbons display strong, sweeping undulose extinction and are locally characterized by well-developed core-and-mantle microstructures (Figure 11b) [*Hirth and Tullis*, 1992]. The thrust-related, phyllonitic mylonites comprise sericite (greater than ~20% by volume), quartz, feldspar, albite, hornblende, actinolite, and epidote. The foliation is defined by polycrystalline quartz ribbons and interconnected aggregates of intensely aligned sericite grains, which enclose relict feldspar and hornblende porphyroclasts (Figure 11c). Thin section observations indicate that the sericite-rich foliae developed because of chemical breakdown of original feldspar grains, by a process similar to that observed in the Uists (e.g., (1), section 3.2.3) [*Imber*, 1998]. Hornblende grains are typically unaltered and are crosscut by arrays of intragranular extension fractures infilled by fibrous, syntectonic quartz-actinolite intergrowths. In deformed metadolerite sheets, transgranular extension fractures are widely developed, particularly adjacent to fold hinge regions, and are infilled by syntectonic quartz-actinolite fibers. These veins are progressively sheared out into the mylonitic foliation as they are traced from the more competent metadolerites into adjacent, less competent quartzo-feldspathic rocks (e.g., Figure 11d).

Microstructural observations show that Proterozoic-age, thrust-related phyllonitization produced a syntectonic mineral

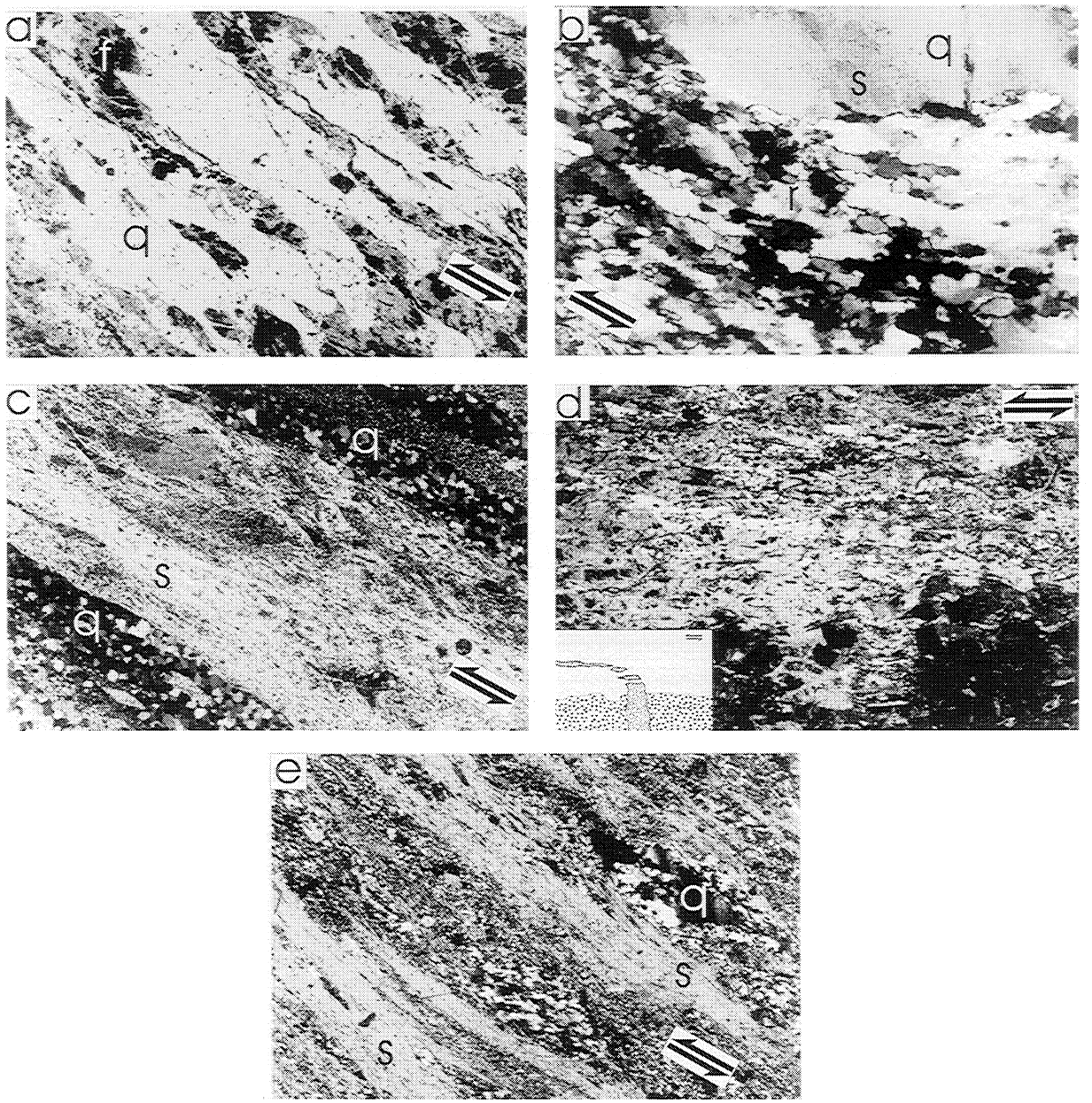

Figure 11. Photomicrographs of fault rocks, Scalpay. (a) Feldspar porphyroclasts (f) "float" in a matrix of interconnected quartz ribbons (q). Split arrows are parallel to mineral lineation, top to NW shear. Field of view is 6 × 3.7 mm, with plane polarized light. (b) Quartz grain (q) with poorly developed optical subgrains (s) surrounded by a mantle of recrystallized quartz (r). Note that the recrystallized quartz grains are flattened and display irregular grain boundary geometries. Split arrows are parallel to mineral lineation, top to NW shear. Field of view is 1.3 × 0.77 mm, with crossed polars. (c) Thrust-related phyllonitic mylonite. The foliation is defined by interconnected sericite strands (s) and polycrystalline quartz ribbons (q). Split arrows are parallel to mineral lineation, top to NW shear. Field of view is 6 × 3.7 mm, with crossed polars. (d) The contact between quartzo-feldspathic mylonite (top) and a deformed metadolerite sheet (bottom). Note that the transcrystalline syntectonic vein appears to be undeformed within the metadolerite sheet, but is progressively sheared to the left within the quartzo-feldspathic mylonite. Split arrows are parallel to mineral lineation, top to NW shear. Field of view is 12 × 7.2 mm, with crossed polars. Inset shows a line drawing of the photomicrograph; metadolerite is coarse stipples, and vein is fine stipples. (e) Strike-slip-related phyllonite. The foliation is defined by an interconnected network of sericite strands (s) and flattened, partially recrystallised quartz ribbons (q). Split arrows are parallel to mineral lineation, top to NE shear. Field of view is 6 × 3.7 mm, with plane polarized light.

assemblage of sericite, albite, actinolite, and epidote. Hornblende and biotite, present in the parent gneisses, coexist with syntectonic actinolite. This association is similar to the transitional upper greenschist to lower amphibolite facies assemblages described in regionally metamorphosed basic rocks by *Miyashiro* [1994], implying that deformation probably occurred at between 400° and 500°C [*Yardley*, 1989]. Our interpretation is consistent, within error, with the estimates of 535° ± 50°C [*Fettes and Mendum*, 1987] and 520° ± 60°C [*White*, 1996] obtained from Proterozoic-age mylonites at Seaforth Head (section 2 and Figures 2 and 3), and suggests that thrust-related phyllonitization probably occurred at temperatures in excess of 500°C. Microstructural observations show that the quartzo-feldspathic and phyllonitic mylonites differ only in the modal sericite content (i.e., in the degree of retrogression). Thus the phyllonitic mylonites appear to represent localized zones of intense, fluid-related alteration and retrogression, which probably developed along strain heterogeneities [e.g., *Thompson and Connolly*, 1992; *Oliver*, 1996] within the Proterozoic shear zone. Once again, we follow the arguments of *Jordan* [1987] and *Handy* [1990] and interpret the bulk rheological behaviour of the quartzo-feldspathic and phyllosilicate-rich mylonites as having been controlled by the deformation response of the interconnected quartz ribbons and sericitic foliae. The presence of elongate quartz ribbons/quartz core-and-mantle microstructures strongly suggest that quartz deformed by intracrystalline, crystal-plastic deformation mechanisms [*Hirth and Tullis*, 1992]. For the same reasons as discussed insection 3.2.3., we believe the sericite-rich foliae to have developed by a combination of grain size-sensitive pressure solution creep and fluid-present crystal-plastic deformation. The abundance of fibrous, syntectonic quartz-actinolite overgrowths and fracture infills (e.g., Figure 11d) strongly suggests that fluid-assisted diffusive mass transfer processes must have been important operative deformation mechanisms during Proterozoic thrusting. From these interpretations we conclude that Proterozoic-age thrusting on Scalpay was accommodated by heterogeneous, viscous flow during upper greenschist to lower amphibolite facies retrogression within packages of quartzo-feldspathic mylonite and phyllonite. Thus deformation and phyllonitization occurred entirely within the viscous flow regime of *Schmid and Handy* [1991]. We infer that at that time the present-day erosion surface on Scalpay must have been below the level of the Proterozoic frictional-viscous transition.

The Caledonian-age strike-slip-related phyllonites from the Cnoc na Croich and Kennavay shear zones comprise a syntectonic mineral assemblage of sericite, chlorite, quartz, albite, epidote, calcite, and opaque minerals (Figure 11e). In contrast to the thrust-related phyllonitic mylonites, hornblende, and actinolite are absent and feldspar porphyroclasts are rarely preserved, implying that strike slip reactivation was associated with intense but highly localised prehenite-pumpellyite to greenschist facies retrogression (see section 3.2.3.). Apart from a higher modal abundance of calcite these Caledonian-age phyllonites are otherwise identical to the phyllonites preserved along the southern segment [*Imber*, 1998]. Thus we infer that Caledonian sinistral strike slip was accommodated by heterogeneous, viscous flow and that the present-day erosion surface on Scalpay was, at that time, below the level of the Caledonian frictional-viscous transition (see section 3.2.3. for discussion).

3.4. Summary

To summarize, field and microstructural observations from both the southern and northern segments of the Outer Hebri-

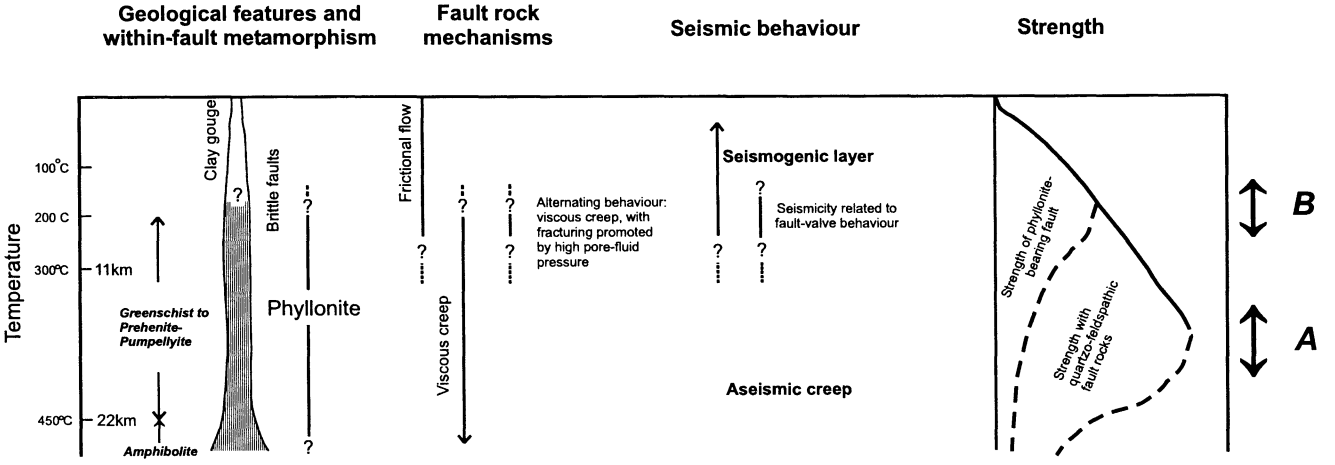

Figure 12. Synoptic shear zone model applicable to the OHFZ and to other crustal-scale faults with shallow, tectonically modified frictional-viscous transition zones, modified from *Scholz* [1988]. Temperature scale refers to temperatures outside the fault zone, while metamorphic facies refer to fluid-related metamorphism within the fault zone. Depth scale is for illustrative purposes only and is taken from *Scholz's* [1988] Figure 4. Consideration of the total exposed thickness of phyllonite compared to the total width of the OHFZ (Figure 2a) suggests that the width of the fault zone around the level of the frictional-viscous transition is narrower than that envisaged by *Scholz* [1988]. Schematic strength curves are loosely based on those by *Janecke and Evans* [1988] and *Wintsch et al.*, [1995]. A is the inferred position of the frictional-viscous transition during Caledonian thrusting, and B is the inferred position of frictional-viscous transition during Caledonian sinistral strike slip in the Outer Hebrides. See text for explanation of other features.

des Fault Zone show that at different times the fault zone exposed at the present-day erosion surface either lay above or below the level of an evolving, paleo-frictional-viscous transition (Figure 12). During Caledonian deformation the onset of viscous creep in rocks previously deforming by frictional flow appears to have been triggered by syntectonic, greenschist facies retrogression (300° – 350°C) and phyllonitization controlled by the influx of aqueous fluids into the fault zone. Data from the Proterozoic shear zone exposed along the northern segment, however, show that phyllonitization also occurred at higher temperatures (> 500°C) in the viscous flow regime. Microstructural observations suggest that the processes of syntectonic retrogression and the onset of grain size-sensitive creep were similar during both high- and low-temperature phyllonitization. So far, however, we have not considered the thermal consequences of deformation, effects which could have important implications for the rheological development of the fault zone. In section 4 we discuss the likely thermal evolution of the OHFZ during Caledonian deformation and consider its impact on the rheology of the fault zone.

4. Discussion

4.1. Thermal History and the Nature of the Frictional-Viscous Transition

Central to our argument is the notion that the observed switch from frictional to viscous flow during Caledonian deformation was controlled by the influx of fluids causing widespread retrogression and phyllonitization in the fault zone. It is important to establish, however, that the change in deformation regime was not caused by a rise in temperature due to either reburial and heating due to Caledonian thrust-related crustal thickening and/or to frictional shear heating of the fault zone.

As noted in section 2, Caledonian thrusting probably thickened the crust in the Outer Hebrides by between 2 and 3 km. Any additional heating arising from crustal thickening could, potentially, have triggered the observed onset of viscous flow by increasing the geothermal gradient and hence raising the level of the frictional-viscous transition relative to the present-day erosion surface. Substantial heating can only be avoided if the rocks are exhumed rapidly, within a few tens of millions of years (< 40 Myr) following burial [*England and Thompson*, 1984].

Two independent lines of evidence suggest that the rocks in the Outer Hebrides were not subjected to significant heating following Caledonian thrusting. Isotopic age dates from a pseudotachylyte vein exposed along the southern segment constrain brittle thrusting (i.e., the onset of burial) across the OHFZ to ca. 430 Ma [*Kelley et al.*, 1994] (section 2). Apatite fission track data, which is used to model sub-110°C cooling histories, show that rocks at the present-day erosion surface in Lewis and Harris had begun to cool from a maximum temperature of ~110°C from the beginning of the Devonian (ca. 400 Ma) or perhaps earlier [*Lewis et al.*, 1992]. These data show that thrusting, strike slip, and some, if not all, of the extension observed onshore took place within a time frame of ~30 Myr, implying that exhumation rates in the Outer Hebrides may have been fast enough to prevent significant burial-related heating. This conclusion is supported by radiometric age dates obtained from gneisses preserved in the footwall of the OHFZ (Figure 3). The youngest Rb-Sr and K-Ar biotite ages are all older than ca. 1100 Ma, even for samples lying within a few hundred meters of the mapped basal fault [e.g., *Cliff and Rex*, 1989, Figure 2]. This observation is consistent with the footwall gneisses having remained at temperatures of less than ~250°–300°C since the close of the Grenvillian tectonothermal event (section 2) and effectively rules out a prolonged episode of burial-related heating of the footwall during Caledonian thrusting. We infer from this that the temperature increase (from ~250°-350°C) within the fault zone during phyllonitization (section 3.2.3) was restricted to the actively deforming zone and, as such, may reflect localized heat advection caused by focused fluid flow along the fault [*Thompson and Connolly*, 1992].

In theory, additional heat could be provided by frictional shear heating along the fault zone during Caledonian thrusting (compare models discussed by *Brun and Cobbold* [1980] and *England and Molnar* [1993]). The widespread occurrence of pseudotachylytes along the OHFZ certainly suggests that localized frictional heating leading to melting was widespread [*Sibson*, 1975, 1977a, 1977b]. However, the development of fabrics consistent with viscous flow is everywhere associated with the onset of later Caledonian strike slip and extensional movements. We therefore see no compelling reason to link localized thrust-related frictional melting processes to a more general heating of the OHFZ.

The overall conclusion to draw from this section is that burial- and shear-related heating cannot have been the primary controls on the observed change from frictional to viscous flow. Instead, we propose that the influx of warm, aqueous fluids into the previously "dry" fault zone triggered widespread retrogression and phyllonitization and caused the Caledonian frictional-viscous transition to migrate upward through the crust within the fault zone relative to the level of the present-day erosion surface (Figure 12). Structural mapping in both northern and southern segments [*Sibson*, 1977b; *Butler*, 1995; *Imber*, 1998] demonstrates that Caledonian-age phyllonites are developed along almost the entire onshore OHFZ (Figure 2a), implying that shallow, tectonically modified frictional-viscous transitions are not isolated phenomena but are features that can, potentially, occur along the length of crustal-scale fault zones. The Proterozoic-age shear zone exposed on Scalpay preserves a section through an older, more deeply exhumed part of the fault zone. The presence of upper greenschist to lower amphibolite facies phyllonites, which record temperatures in excess of > 500°C, shows that fluid influx, retrogression, and phyllonitization also occurred within the viscous flow regime and implies that Caledonian-age or older phyllonites could, potentially, occur over a wide depth range within the fault zone. Thus, our study provides an observational basis for recent models which, using limited data, postulated that the development of phyllosilicate-rich fault rocks and/or the operation of grain size-sensitive deformation mechanisms could lead to extreme shallowing of the frictional-viscous transition [*Wintsch et al.*, 1995; *Stewart et al.*, 2000; *Holdsworth et al.*, 2001].

The midcrustal parts of large, crustal-scale faults like the OHFZ typically lie within the pressure-temperature (P-T) range that favors (1) greenschist facies retrogression to fine-grained phyllosilicate aggregates and (2) the operation of fluid-assisted diffusive mass transfer processes. We suggest

that provided large volumes of fluid are available and that the fault/shear zone network can act as a fluid pathway [e.g., *Oliver*, 1996], fluid-assisted shallowing of the frictional-viscous transition zone probably occurs along many other mature, crustal-scale fault zones (e.g., the Great Glen Fault Zone; Figure 2a, inset) [*Stewart et al.*, 1999, 2000; *Holdsworth et al.*, 2001]. Moreover, the Outer Hebrides Fault Zone preserves evidence for multiple phyllonitization events, separated by long (hundreds of Myr) periods without retrogression. This is consistent with the development of shallow, tectonically modified frictional-viscous transition zones being a characteristic process that occurs many times during the life of strongly reactivated structures. On the basis of our studies of the OHFZ we propose that basement faults characterized by an early phase of intense, brittle deformation will be very susceptible to fluid influx and are therefore most likely to display modified frictional-viscous transitions.

The interpretation of the OHFZ presented here apparently conflicts with that of *White* [1996], who using paleopiezometric estimates of the differential stresses developed within a segment of the Proterozoic shear zone exposed at Seaforth Head (Figure 2), inferred that the frictional-viscous transition during westward directed overthrusting occurred at ~16 km depth. Significantly, there is little evidence for syntectonic retrogression or veining within the mylonite belt exposed at Seaforth Head [*Walker*, 1990; *Imber*, 1998], consistent with thrusting having locally occurred under fluid-deficient conditions [*White*, 1996]. In such "dry" environments, fluid-assisted diffusive mass transfer and/or syntectonic retrogression will be suppressed, and the depth to the frictional-viscous transition is likely to be controlled primarily by the geothermal gradient and strain rate. Thus in those parts of a fault zone where fluids are absent a normal depth frictional-viscous transition zone (in the sense of *Sibson* [1977a, 1983] and *Scholz* [1988]) is likely to develop. These observations serve to highlight the importance of syntectonic fluid-rock interaction in controlling the structural evolution of midcrustal faults and shear zones [*White*, 1996; *Stewart et al.*, 2000].

4.2. Implications for Seismicity and Heat Flow Along Crustal-Scale Faults

In addition to any possible long-term (i.e., geologically observed) mechanical weakening effects operating on the scale of the fault zone (Figure 12) (see *Stewart et al.* [2000], *Holdsworth et al.* [2001] and *Walsh et al.* [2001] for discussion), the development of shallow, tectonically modified frictional-viscous transition zones is likely to have major implications for the geophysical properties of crustal-scale faults such as seismicity and surface heat flow. *Wintsch et al.* [1995] proposed that aseismic slip may be a characteristic of faults containing localised concentrations of phyllosilicate-bearing fault rocks. While this assertion may be true of some faults, our observations from the Outer Hebrides Fault Zone suggest otherwise. Field relationships demonstrate that extensional reactivation of the phyllonitic shear zones on North Uist (section 3.2.1) was accommodated by macroscopically ductile, viscous flow, alternating with brittle faulting and vein emplacement both within and along the shear zone margins. Several generations of crosscutting and foliation-parallel syntectonic veins are recognized, consistent with *Sibson's* [1990] model of fault valve behavior in which short-lived hydraulic fracturing and fault zone embrittlement events alternated with longer-lived phases of low-temperature ductile shearing. We suggest that the abundance of strongly aligned phyllosilicates within and around the actively deforming shear zones may have provided a low-permeability "seal", thus promoting fault valve behavior around the level of the frictional-viscous transition at depths corresponding to within-fault temperatures of between 300° and 350°C. Further work is needed to test this model, but if it is correct, it implies that seismic deformation is likely to be a characteristic feature of phyllosilicate-bearing faults with shallow frictional-viscous transitions (Figure 12). In such a system the exact depth of the seismogenic layer [*Scholz*, 1990] may vary systematically in both space and time and, in addition to parameters such as strain rate and geothermal gradient, is likely to be influenced by both the degree of phyllonitization and the pore fluid pressure developed within the fault zone around the level of the shallowed frictional-viscous transition.

The amount of frictional heat generated by movement along a fault is proportional to its long-term slip rate multiplied by the frictional resistance to sliding on the fault plane. For high mean values of frictional resistance (stresses of 50–100 MPa) a positive heat flow anomaly centered over the fault is expected to develop [*Lachenbruch and Sass*, 1992]. Standard calculations assume that the absence of a positive heat flow anomaly means either that the fault is filled with very weak, low- friction material [e.g., *Shimamoto and Logan*, 1981] or that the fault core is highly overpressured and therefore moves under low effective normal stresses [e.g., *Rice*, 1992]. As frictional resistance increases with depth, any heat flow observed at the Earth's surface will be influenced by the depth to which the fault deforms by predominantly frictional sliding in the hydrostatic stress regime, i.e. by the depth of the frictional-viscous transition [e.g., *Lachenbruch and Sass*, 1980, equation (A23b)]. If, as implied by our findings in the Outer Hebrides, the transition occurs at shallow depths, then the total frictional resistance developed along that fault is likely to be lower than if the frictional-viscous transition is assumed to be at 10–15 km depth. We suggest therefore that faults with shallow, tectonically modified frictional-viscous transition zones may be characterized by heat flow anomalies that are lower than those predicted assuming a normal depth transition [e.g., *Lachenbruch and Sass*, 1992, Figure 7b]. In other words, low heat flow anomalies are not necessarily diagnostic of low friction gouges or overpressured frictional fault cores but may imply that phyllosilicate-bearing mylonites exist at shallow depths within the crust (Figure 12).

5. Conclusions

Our study of the Outer Hebrides Fault Zone highlights the importance of fluid-rock interaction in mature, crustal-scale fault zones and provides an observational basis for recently published rheological models. In particular, we have shown the following.

1. The present-day fault rock distribution along the southern segment of the Outer Hebrides Fault Zone preserves evidence for a shallow, tectonically modified frictional-viscous transition zone. Contrary to *Sibson's* [1977a] interpretation, it does not represent an asymmetrically exhumed depth section through the continental crust.

2. Shallowing of the frictional-viscous transition was ultimately controlled by the syntectonic influx of aqueous fluids along preexisting heterogeneities (brittle fractures and contrasts in ductile strain) within the fault zone, triggering fluid-assisted diffusive mass transfer and phyllonitization across a broad depth range in both frictional and viscous flow regimes.

3. Phyllonitization occurred at several different times during the period of activity along the Outer Hebrides Fault Zone, with ~700 Myr separating Proterozoic-age, thrust-related phyllonitization on Scalpay from dip-slip-related, Late Caledonian phyllonitization on the Uists. Still younger phyllonites may have formed at depths down to the present day midcrust during post-Caledonian dip-slip reactivation episodes. This implies that shallow, tectonically modified frictional-viscous transition zones are semi-permanent features within many long-lived continental fault zones.

4. If major fault zones are able to act as effective fluid pathways, then the midcrustal sections will almost inevitably be affected by reaction softening and the onset of grain size-sensitive creep since the pressure-temperature conditions are particularly favorable to the operation of these processes. As such, the development of shallow, tectonically modified transition zones may be a characteristic process within long-lived continental basement faults.

Finally, we tentatively propose that faults with shallow, tectonically modified frictional-viscous transition zones may be characterized by lower average frictional stresses and surface heat flow anomalies compared to other fault zones. Thus an explanation for the stress-heat flow paradox and apparent weakness of the San Andreas fault [e.g., *Zoback*, 2000] may ultimately be found by studying ancient fault zone processes in the exhumed sections of equivalent-scale reactivated fault zones.

Acknowledgments. We gratefully acknowledge funding from the U.K. Natural Environment Research Council (studentship GT4/94/146/G to J.I.) and Amerada Hess Ltd. (R.E.H. and studentship to C.A.B.). The authors thank Ian Main (Edinburgh) and colleagues in the Fault Analysis Group (Dublin) for discussions that helped to clarify several of the concepts outlined in this paper. We are grateful to G. Axen, D. Cowan, and N. Mancktelow for thorough and constructive reviews leading to significant improvements in the structure of our arguments. Lee Watts and K. Atkinson are thanked for their help with the photographic figures. T. Holding and T. Lapworth are thanked for assistance in the field.

References

Binns, P. E., R. McQuillin, and N. Kenolty, The geology of the Sea of the Hebrides, *Rep. 73/14*, 44 pp., Inst. Geol. Sci., HMSO, London, 1974.

Brodie, J., and N. White, Sedimentary basin inversion caused by igneous underplating– Northwest European continental shelf, *Geology, 22*, 147-150, 1994.

Brun, J. P., and P. R. Cobbold, Strain heating and thermal softening in continental shear zones: A review, *J. Struct. Geol., 2*, 149-158, 1980.

Burkhard, M., Calcite twins, their geometry, appearance and significance as stress-strain markers and indicators of tectonic regime: A review, *J. Struct. Geol., 15*, 351-368, 1993.

Butler, C. A., Basement fault reactivation: The kinematic evolution of the Outer Hebrides Fault Zone, Scotland, Ph.D. thesis, Univ. of Durham, Durham, England, 1995.

Butler, C. A., R. E. Holdsworth, and R. A. Strachan, Evidence for Caledonian sinistral strike-slip and associated fault zone weakening, Outer Hebrides Fault Zone, Scotland, *J. Geol. Soc. London, 152*, 743-746, 1995.

Cliff, R. A., and D. C. Rex, Evidence for a "Grenville" event in the Lewisian of the northern Outer Hebrides, *J. Geol. Soc. London, 146*, 921-924, 1989.

Coward, M. P., The structural and metamorphic geology of South Uist, Outer Hebrides, Ph.D. thesis, Univ. of London, London, England, 1969.

Coward, M. P., The Eastern Gneisses of South Uist, *Scott. J. Geol., 8*, 1-12, 1972.

Drury, M. R., and J. L. Urai, Deformation-related recrystallisation processes, *Tectonophysics, 172*, 235-253, 1990.

Engelder, T., Cataclasis and the generation of fault gouge, *Bull. Geol. Soc. Am., 85*, 1515-1522, 1974.

England, P., and P. Molnar, The interpretation of inverted metamorphic isograds using simple physical calculations, *Tectonics, 12*, 145-157, 1993.

England, P. C., and A. B. Thompson, Pressure-temperature-time paths of regional metamorphism, I., Heat transfer during the evolution of regions of thickened continental crust, *J. Petrol., 25*, 894-928, 1984.

Fettes, D. J., and J. R. Mendum, The evolution of the Lewisian complex in the Outer Hebrides, in *Evolution of the Lewisian and Comparable Precambrian High Grade Terrains*, edited by R. G. Park and J. Tarney, *Geol. Soc. Spec. Publ., 27*, 1987.

Fettes, D. J., J. R. Mendum, D. I. Smith, and J. V. Watson, *Geology of the Outer Hebrides*, 198 pp., memoir of the British Geological Survey, Sheets (solid edition) Lewis and Harris, Uist and Barra (Scotland), HMSO, London, 1992.

Fowler, C. M. R., *The Solid Earth*, 472 pp., Cambridge Univ. Press, New York, 1990.

Goodwin, L. B., and H.-R. Wenk, Development of phyllonite from granodiorite: Mechanisms of grain-size reduction in the Santa Rosa mylonite zone, California, *J. Struct. Geol., 17*, 689-707, 1995.

Grocott, J., The relationship between Precambrian shear belts and modern fault systems, *J. Geol. Soc. London, 133*, 257-261, 1977.

Guermani, A., and G. Pennacchioni, Brittle precursors of plastic deformation in a granite: An example from the Mont Blanc massif (Helvetic, western Alps), *J. Struct. Geol., 20*, 135-148, 1998.

Handy, M. R., Deformation regimes and the rheological evolution of fault zones in the lithosphere: The effects pressure, temperature, grainsize and time, *Tectonophysics, 163*, 119-152, 1989.

Handy, M. R. The solid-state flow of polymineralic rocks, *J. Geophys. Res.*, 95, 8647-8661, 1990.

Hippertt, J. F., Microstructures and *c*-axis fabrics indicative of quartz dissolution in sheared quartzites and phyllonites, *Tectonophysics, 229*, 141-163, 1994a.

Hippertt, J. F., Direct observation of porosity in quartzite and phyllonite, *Neues Jahrb. für Mineral., 166*, 239-259, 1994b.

Hippertt, J. F., Breakdown of feldspar, volume gain and lateral mass transfer during mylonitization of granitoid in a low metamorphic grade shear zone, *J. Struct. Geol., 20*, 175-193, 1998.

Hirth, G., and J. Tullis, Dislocation creep regimes in quartz aggregates, *J. Struct. Geol., 14*, 145-159, 1992.

Holdsworth, R. E., C. A. Butler, and A. M. Roberts, The recognition of reactivation during continental deformation, *J. Geol. Soc. London, 154*, 73-78, 1997.

Holdsworth, R. E., M. Stewart, J. Imber, and R. A. Strachan, The structure and rheological evolution of reactivated continental fault zones: A review and case study, in *Continental Reactivation and Reworking*, edited by J.A. Miller, R.E. Holdsworth, I. S. Buick, and M. Hand, *Geol. Soc. Spec. Publ., 184*, 115-137, 2001.

Imber, J., Deformation and fluid-rock interaction along the reactivated Outer Hebrides Fault Zone, Scotland, Ph.D. thesis, Univ. of Durham, Durham, England, 1998.

Imber, J., R. E. Holdsworth, C. A. Butler, and G. E. Lloyd, Fault-zone weakening processes along the reactivated Outer Hebrides Fault Zone, Scotland, *J. Geol. Soc. London, 154*, 105-109, 1997.

Janecke, S. U., and J. P. Evans, Feldspar-influenced rock rheologies, *Geology, 16*, 1064-1067, 1988.

Jordan, P. G., The deformational behaviour of bimineralic limestone-halite aggregates, *Tectonophysics, 135*, 185-197, 1987.

Kelley, S. P., S. M. Reddy, and R. H. Maddock, Laser-probe $^{40}Ar/^{39}Ar$ investigation of a pseudotachylyte and its host rock from the Outer Isles thrust, Scotland, *Geology, 22*, 443-446, 1994.

Knipe, R. J., Deformation mechanisms-recognition from natural tectonites, *J. Struct. Geol., 11*, 127-146, 1989.

Lachenbruch, A. H., and J. H. Sass, Heat flow and energetics of the San Andreas Fault Zone, *J. Geophys. Res., 85*, 6185-6222, 1980.

Lachenbruch, A. H., and J. H. Sass, Heat flow from Cajon Pass, fault strength, and tectonic implications, *J. Geophys. Res., 97*, 4995-5015, 1992.

Lailey, M., A. M. Stein, and T. J. Reston, The Outer Hebrides Fault: A major Proterozoic structure in NW Britain, *J. Geol. Soc. London, 146*, 253-259, 1989.

Lambert, R. St. J., J.S. Myers and J.V.Watson, An apparent age for a member of the Scourie dyke suite in Lewis, Outer Hebrides. *Scott. J. Geol.*, 6, 214-220, 1970.

Lewis, C. L. E., A. Carter, and A. J. Hurford, Low-temperature effects of the Skye Tertiary intru-

sions on Mesozoic sediments in the Sea of Hebrides Basin, in *Basins on the Atlantic Seaboard: Petroleum Geology, Sedimentology and Basin Evolution*, edited by J. Parnell, *Geol. Soc. Spec. Publ., 62*, 175-188, 1992.

Lisle, R. J., Strike-slip motion in the Minches, NW Scotland, *J. Geol. Soc. London, 150*, 653-656, 1993.

Lloyd, G. E., and R. J. Knipe, Deformation mechanisms accommodating faulting of quartzite under upper crustal conditions, *J. Struct. Geol., 14*, 127-143, 1992.

MacInnes, E. A., G. I. Alsop, and G. J. H. Oliver, Contrasting modes of reactivation in the Outer Hebrides Fault Zone, northern Barra, Scotland *J. Geol. Soc. London, 157*, 1009-1017, 2000.

Maltman, A., Prelithification deformation in *Continental Deformation*, edited by P. L. Hancock, pp. 143-158, Pergamon, Tarrytown, N.Y., 1994.

Mares, V. M., and A. K. Kronenberg, Experimental deformation of muscovite, *J. Struct. Geol., 15*, 1061-1075, 1993.

McCaig, A. M., and R. J. Knipe, Mass-transport mechanisms in deforming rocks: Recognition using microstructural and microchemical criteria, *Geology, 18*, 824-827, 1990.

Miyashiro, A., *Metamorphic Petrology*, 404 pp., University College London Press, London, 1994.

Moorbath, S., J. L. Powell, and P. N. Taylor, Isotopic evidence for the age and origin of the "grey gneiss" complex of the southern Outer Hebrides, Scotland, *J. Geol. Soc. London, 131*, 213-222, 1975.

O'Hara, K., Fluid flow and volume loss during mylonitization: An origin for phyllonite in an overthrust setting, North Carolina, USA, *Tectonophysics, 156*, 21-36, 1988.

Oliver, N. H. S., Review and classification of structural controls on fluid flow during regional metamorphism, *J. Metamorph. Geol., 14*, 477-492, 1996.

Osinski, G. R., G. I. Alsop, and G. J. H. Oliver, Extensional tectonics of the Outer Hebrides Fault Zone, South Uist, NW Scotland, *Geol. Mag.*, in press, 2001.

Peddy, C. P. Displacement of the Moho by the Outer Isles Thrust shown by seismic modelling, *Nature, 312*, 628-630, 1984.

Pidgeon, R. T., and M. A. Aftalion, The geochronological significance of discordant U-Pb ages of oval-shaped zircons from a Lewisian Gneiss from Harris, *Earth Planet. Sci. Lett., 17*, 269-274, 1972.

Piper, J. D. A., Post-Laxfordian magnetic imprint in the Lewisian metamorphic complex and strike-slip motion in the Minches, NW Scotland, *J. Geol. Soc. London, 149*, 127-137, 1992.

Pryer, L. L., and P.-Y. F. Robin, Retrograde metamorphic reactions in deforming granites and the origin of flame perthites, *J. Metamorph. Geol., 13*, 645-658, 1995.

Rice, J. R., Fault stress, pore pressure distributions, and the weakness of the San Andreas Fault in *Fault Mechanics and Transport Properties of Rocks*, edited by B. Evans and T.-F. Wong, 475-503, Academic, San Diego, Calif., 1992.

Roberts, A. M., and R. E. Holdsworth, Linking onshore and offshore structures: Mesozoic extension in the Scottish Highlands, *J. Geol. Soc. London 156*, 1061-1064, 1999.

Rutter, E. H., Pressure solution in nature, theory and experiment, *J. Geol. Soc. London, 140*, 725-740, 1983.

Rutter, E. H., R.E. Holdsworth, and R. J. Knipe, The nature and tectonic significance of fault zone weakening: An introduction, in *The Nature and Tectonic Significance of Fault Zone Weakening*, edited by R. E. Holdsworth et al., *Geol. Soc. Spec. Publ., 186*, 1-11, 2001.

Schmid, S. M., and M. R. Handy, Towards a genetic classification of fault rocks: Geological usage and tectonophysical implications, in *Controversies in Modern Geology: Evolution of Geological Theories in Sedimentology, Earth History and Tectonics*, edited by D. W. Müller, J. A. McKenzie, and H. Weissert, pp. 339-361, Academic, San Diego, Calif., 1991.

Scholz, C. H., The brittle-plastic transition and the depth of seismic faulting, *Geol. Rundsch., 77*, 319-328, 1988.

Scholz, C. H., *The Mechanics of Earthquakes and Faulting*, 439 pp., Cambridge Univ. Press, New York, 1990.

Shea, W. T., and A. K. Kronenberg, Rheology and deformation mechanisms of isotropic mica schist, *J. Geophys. Res., 97*, 15,201-15,237, 1992.

Shimamoto, T., and J. M. Logan, Effects of simulated clay gouges on the sliding behaviour of Tennessee sandstone, *Tectonophysics, 75*, 243-255, 1981.

Sibson, R. H., Generation of pseudotachylyte by ancient seismic faulting, *Geophys. J. R. Astron. Soc., 43*, 775-794, 1975.

Sibson, R. H., Fault rocks and fault mechanisms, *J. Geol. Soc. London, 133*, 191-213, 1977a.

Sibson, R. H., The Outer Hebrides Thrust: Its structure, mechanism and deformation environment, Ph.D. thesis, Univ. of London, London, England, 1977b.

Sibson, R. H., Fault zone models, heat flow, and the depth distribution of earthquakes in the continental crust of the United States, *Bull. Seismol. Soc. Am., 72*, 151-163, 1982.

Sibson, R. H., Continental fault structure and shallow earthquake source, *J. Geol. Soc. London, 140*, 741-767, 1983.

Sibson, R. H., Conditions for fault-valve behaviour, in *Deformation Mechanisms, Rheology and Tectonics*, edited by R. J. Knipe, and E. H. Rutter, *Geol. Soc. Spec. Publ., 54*, London, 15-28, 1990.

Skelton, A. D. L., C. M. Graham, and M. J. Bickle, Lithological and structural controls on regional 3-D fluid flow patterns during greenschist facies metamorphism of the Dalradian of the SW Scottish Highlands, *J. Petrol., 36*, 563-586, 1995.

Smythe, D. K., A. Dobinson, R. McQuillin, J. A. Brewer, D. H. Matthews, D. J. Blundell, and B. Kelk, Deep structure of the Scottish Caledonides revealed by the MOIST reflection profile, *Nature, 299*, 338-340, 1982.

Snoke, A. W., J. Tullis, and V. R. Todd (Eds.), *Fault-Related Rocks: A Photographic Atlas*, 613 pp., Princeton Univ. Press, Princeton, N.J., 1988.

Steel, R. J., and A. C. Wilson, Sedimentation and tectonism (?Permo-Triassic) on the margin of the North Minch Basin, Lewis, *J. Geol. Soc. London, 131*, 183-202, 1975.

Stein, A. M., Basement controls upon basin development in the Caledonian foreland, *Basin Res., 1*, 107-119, 1988.

Stein, A. M., Basin development and petroleum potential in The Minches and Sea of the Hebrides Basins, in *Basins on the Atlantic Seaboard: Petroleum Geology, Sedimentology and Basin Evolution*, edited by J. Parnell, *Geol. Soc. Spec. Publ., 62*, 17-20, 1992.

Stewart, M., R. A. Strachan, and R. E. Holdsworth, The structure and early kinematic history of the Great Glen Fault Zone, Scotland, *Tectonics, 18*, 326-342, 1999.

Stewart, M., R. E. Holdsworth, and R. A. Strachan, Deformation processes and weakening mechanisms within the frictional-viscous transition zone of major crustal-scale faults: Insights from the Great Glen Fault Zone, Scotland, *J. Struct. Geol., 22*, 543-560, 2000.

Strachan, R. A., and R. E. Holdsworth, Proterozoic sedimentation, orogenesis and magmatism on the Laurentian Craton (2500 – 750 Ma), in *Geological History of Britain and Ireland*, edited by N. H. Woodcock and R. A. Strachan, pp. 52-72, Blackwell Sci., New York, 2000.

Thompson, A. B., and J. A. D. Connolly, Migration of metamorphic fluid: Some aspects of mass and heat transfer, *Earth Sci. Rev., 32*, 107-121, 1992.

Thomson, K., J. R. Underhill, P. F. Green, R. J. Bray, and H. J. Gibson, Evidence from apatite fission track analysis for the post-Devonian burial and exhumation history of the northern Highlands, Scotland, *Mar. Petrol. Geol., 16*, 27-39, 1999.

Tourigny, G., and A. Tremblay, Origin and incremental evolution of brittle/ductile shear zones in granitic rocks: Natural examples from the southern Abitibi Belt, Canada, *J. Struct. Geol., 19*, 15-27, 1997.

Tullis, J., and R. A. Yund, Hydrolytic weakening of experimentally deformed Westerly granite and Hale albite rock, *J. Struct. Geol., 2*, 439-451, 1980.

van Breemen, O., M. Aftalion, and R. T. Pidgeon, The age of the granitic injection complex of Harris, Outer Hebrides, *Scott. J. Geol., 7*, 139-152.

Walker, J., A study of the deformation environment of the Outer Hebrides Fault Zone, Ph.D. thesis, Univ. of London, London, England, 1990.

Walsh, J. J., et al., Geometrical controls on the evolution of normal fault systems, in *The Nature and Tectonic Significance of Fault Zone Weakening*, edited by R. E. Holdsworth et al., *Geol. Soc. Spec. Publ., 186*, 157-170, 2001.

Watson, J., The Outer Hebrides: A geological perspective, *Proc. Geol. Assoc., 88*, 1-14, 1977.

White, J. C., Transient discontinuities revisited: Pseudotachylyte, plastic instability and the influence of low pore fluid pressure on deformation processes in the mid-crust, *J. Struct. Geol., 18*, 1471-1486, 1996.

White, S. H., and J. Glasser, The Outer Hebrides Fault Zone: Evidence for normal movements, in *Evolution of the Lewisian and Comparable Precambrian High Grade Terrains*, edited by R. G. Park and J. Tarney, *Geol. Soc. Spec. Publ., 27*, 175-183, 1987.

White, S. H., P. G. Bretan, and E. H. Rutter, Fault-zone reactivation: Kinematics and mechanisms, *Phil. Trans. R. Soc., London, ser. A317*, 81-97, 1986.

Whitehouse, M. J., Age of the Corodale Gneisses, South Uist, *Scott. J. Geol., 29*, 49-58, 1993.

Wibberley, C., Are feldspar-to-mica reactions necessarily reaction-softening processes in fault zones?, *J. Struct. Geol., 21*, 1219-1227, 1999.

Wintsch, R. P., R. Christofferson, and A. K. Kronenberg, Fluid-rock reaction weakening of fault zones, *J. Geophys. Res., 100*, 13,021-13,032, 1995.

Yardley, B. W. D., *An Introduction to Metamorphic Petrology*, 248 pp., John Wiley, New York, 1989.

Zoback, M. D., Strength of the San Andreas, *Nature, 405*, 31-32, 2000.

C. A. Butler and R. E. Holdsworth, Reactivation Research Group, Department of Geological Sciences, University of Durham, Durham, DH1 3LE, England, UK. (R.E.Holdsworth@durham.ac.uk)

J. Imber, Fault Analysis Group, Department of Geology, University College Dublin, Belfield, Dublin 4, Ireland (jonathan@fag.ucd.ie)

R. A. Strachan, Geology (BMS), Oxford Brookes University, Headington, Oxford OX3 0BP, England, UK.

(Received July 12, 2000;
Revised April 9, 2001;
Accepted May 7, 2001.)